

The Production of Temperatures Below 1°K by the Adiabatic Demagnetization of 50% $\text{Ce}(\text{PO}_3)_3$ - $\text{Ba}(\text{PO}_3)_2$ Glass

EDWIN LEWIS ALTHOUSE

Solid State Division

July 15, 1968



NAVAL RESEARCH LABORATORY
Washington, D.C.



CONTENTS

Abstract	iii
Problem Status	iii
Authorization	iii
INTRODUCTION	1
Cooling by Adiabatic Demagnetization	1
Problems Associated with Magnetic Cooling	1
Purpose of this Research	1
THEORETICAL BACKGROUND	3
Theory of Magnetic Cooling	3
Low-Temperature Paramagnetism	6
Suitable Cooling Materials	11
EXPERIMENTAL BACKGROUND	11
Temperature Measurement	11
Thermal Contact at Low Temperatures	13
Ce(PO ₃) ₃ -Ba(PO ₃) ₂ GLASS	14
Known Properties	14
Choice of 50% Ce(PO ₃) ₃ -Ba(PO ₃) ₂	15
APPARATUS	15
Exchange Gas System	15
Specimens	16
Susceptibility Measurement Circuit	17
The Dewar	18
The Magnet	18
EXPERIMENTAL PROCEDURE	18
Density Measurement	18
Specimen Analysis	18
Curie Constant Measurement	18
Adiabatic Demagnetization	18
EXPERIMENTAL RESULTS	19
Density	19
Specimen Analysis	19
Curie Constant	19
Temperatures Produced from Different H/T 's	19
$T^{\circ}-T$ Correlation	20
Warmup	26

DISCUSSION OF RESULTS	26
Density	26
Curie Constant	26
Temperatures Produced from Different H/T 's	29
$T^{\circ}-T$ Correlation	32
Warmup	34
SUMMARY	35
ACKNOWLEDGMENTS	35
REFERENCES	36
APPENDIX A - Magnetic Field Dependence of the Heat Capacity	37
APPENDIX B - Time Response of the CMN Thermometer as Determined by the T^3 Thermal Contact Law	38
APPENDIX C - Absolute Determination of the Temperature Scale for a Paramagnetic Material	39

ABSTRACT

The technique of adiabatic demagnetization, also known as "magnetic cooling," for producing low temperatures has been in existence since 1933. Over the years a multitude of coolant materials has been discovered, but most of them are in the form of hydrated paramagnetic salts. Nonhydrous materials have the advantage of greater chemical stability; however, to the author's knowledge, none of the few nonhydrous paramagnetic materials previously investigated are capable of producing temperatures below 0.1°K .

It was the object of this investigation to determine whether cerium metaphosphate glass (specifically 50% by weight $\text{Ce}(\text{PO}_3)_3$ - $\text{Ba}(\text{PO}_3)_2$) is a suitable coolant material for adiabatic demagnetization experiments. Cerium glass is not susceptible to dehydration and attack by glycerine (used for thermal contact) as are many of the hydrated salts. In addition, the concentration of magnetic atoms can be varied over a wide range by diluting the magnetic glass $\text{Ce}(\text{PO}_3)_3$ with the nonmagnetic glass $\text{Ba}(\text{PO}_3)_2$.

The principal results of this investigation are: (a) the 50% $\text{Ce}(\text{PO}_3)_3$ - $\text{Ba}(\text{PO}_3)_2$ glass was successfully cooled many times by adiabatic demagnetization, and "magnetic" temperatures as low as 0.0069°K were reached, (b) using a cerium magnesium nitrate paramagnetic salt as a thermometer, absolute temperatures as low as 0.02°K were observed, and (c) within experimental error, the measured Curie constant for the cerium glass (density 3.57) agrees with that calculated from the Brillouin function for $J = 1/2$ and $1.97 \leq g \leq 2.00$.

PROBLEM STATUS

This is a final report on the problem. Unless otherwise notified, the problem will be considered closed 30 days after the issuance of this report.

AUTHORIZATION

NRL Problem P05-02
Project RR 002-10-45-5051

Manuscript submitted February 9, 1968.

THE PRODUCTION OF TEMPERATURES BELOW 1°K BY THE ADIABATIC DEMAGNETIZATION OF 50% $\text{Ce}(\text{PO}_3)_3$ - $\text{Ba}(\text{PO}_3)_2$ GLASS

INTRODUCTION

Cooling by Adiabatic Demagnetization

To produce temperatures lower than those which can be obtained by pumping on liquid He^4 (0.7 to 0.9°K), one often resorts to the use of systems which remain partially disordered at these temperatures and which can be ordered by a change in some physical parameter. It was pointed out in 1927 by Giauque, and independently in 1926 by Debye, that certain paramagnetic salts constitute systems of this kind because they contain magnetic dipoles which are disordered and which only weakly interact at temperatures around 1°K. They proposed, therefore, that the temperature of such a salt could be lowered below 1°K by successive isothermal magnetization and adiabatic demagnetization. The feasibility of the technique was first demonstrated in 1933 by Giauque and MacDougall at Berkeley and by deHass, Wiersma, and Kramers at Leiden.

Problems Associated with Magnetic Cooling

The limit to which one can cool a paramagnetic material by adiabatic demagnetization is determined by the separation of the lowest energy levels. The smaller the separation, the lower the ultimate temperature that can be reached.

The intrinsic magnetic interactions are controlled by the strength and separation of the dipole moments. The quest for lower temperatures has forced the experimenter to use magnetically dilute materials. The price is paid by an at-least-proportional decrease in the heat capacity.

The stability of the magnetic material with respect to the experimental conditions is also an important criterion to be satisfied. The dehydration and chemical activity of many common coolant materials have been a hindrance to many experimenters.

Purpose of this Research

Interest was aroused in the possible use of cerium-barium metaphosphate (CBP) glass as a material for magnetic cooling because of its greater chemical stability and magnetic dilution capability when compared to most materials in current use. Referring to the list of commonly used materials (Table 1), it appears that only the hydrated salts are capable of producing temperatures below 0.1°K. By surrounding the magnetic ion, the crystalline waters of hydration tend to magnetically dilute the salt, resulting in small dipole-dipole interactions. However, there are specific instances in which the nonhydrated cerium glass can be used with advantage.

When using hydrated salts one must exercise precautions to prevent dehydration, since such a reaction seriously affects the magnetic properties. At room temperature it is often desirable to evacuate the interior of apparatus containing hydrated salts for leak-testing purposes. Such an environment, although abusive to hydrated salts, is completely tolerated by the CBP glass, because it contains no water of hydration. It was believed

Table 1
Paramagnetic Materials Commonly Used in Magnetic Cooling

Hydrated Crystals	Lowest Temperature Obtainable (°K)	Nonhydrous Crystals	Lowest Temperature Obtainable (°K)
Manganous ammonium sulfate	0.15	Ferric acetylacetonate	0.38
Gadolinium sulfate	0.20		
Copper sulfate	0.24		
Ferric ammonium alum	0.04	Ammonium hexafluorochromite	0.10
Ferric methylammonium alum	0.17		
Chrome potassium alum	0.008		
Chrome methylammonium alum	0.013	Synthetic ruby	0.10
Cerium ethyl sulfate	0.03		
Copper potassium sulfate	0.05		
Cerium magnesium nitrate	0.001		

that the glass with appropriate cerium concentration would produce temperatures below 0.1°K.

It is a common procedure to prepare a specimen for adiabatic demagnetization by putting finely powdered paramagnetic salt into a water-glycerine slurry. The water-glycerine slurry is used to provide a more intimate thermal contact between the salt and a system of copper wires or fins which thermally link the coolant to the material under investigation. In chromium potassium alum (CPA), probably the most commonly used salt to produce temperatures near 0.01°K, it has been observed that glycerine causes a decomposition, at room temperature, in which the magnetic properties are adversely affected. Such activity with glycerine would not be expected in the CBP glass.

As previously mentioned, a copper wire or fin system is frequently used as a link to thermally connect the material under investigation to the coolant. A corrosion of the copper wire surface, when embedded in CPA, has been observed. Such a reaction with copper wires is not anticipated at room temperature with the CBP glass, due to its comparative chemical inertness.

The concentration of magnetic ions N in a given paramagnetic material greatly influences the lowest temperature that can be obtained after adiabatic demagnetization. Those materials with smaller concentrations generally cool to lower temperatures than those with larger concentrations. A maximum in the heat capacity occurs near the lowest temperature producible for the material, this limit being largely determined by dipole-dipole interactions. From an experimental point of view it is advantageous to vary N such that the heat capacity maximum falls in the temperature range of interest to approximate nearly isothermal conditions. This is explained later. It is not easy to vary N in the usual salts, except by using different salts. Even then, N is not continuously variable. However, by solution-diluting the magnetic glass $\text{Ce}(\text{PO}_3)_3$ with the non-magnetic glass $\text{Ba}(\text{PO}_3)_2$, N can be varied over a wide range (0 to $5.65 \times 10^{21} \text{ Ce}^{3+}$ ions/cm³).

The absence of hyperfine interactions, as well as the probable absence of Stark interactions below 1°K in cerium compounds, suggests that the magnetic susceptibility would follow Curie's law ($\chi \propto 1/T$) to very low temperatures. This is a most desirable property if the glass is to be used as a thermometer as well as a coolant. A very good agreement with Curie-law behavior has been observed (1-4) in the hydrated salt cerium magnesium nitrate (CMN).

Previously reported properties of $\text{Ce}(\text{PO}_3)_3$ are summarized in the fourth section of the present report. The purpose of this research was to confirm experimentally that the very stable, nonhydrous 50% CBP glass could be cooled to temperatures below 0.1°K and to obtain some estimate of the agreement between the absolute temperature and the temperature corresponding to the magnetic susceptibility of the glass.

The experiments were confined to measurements on glass of a single cerium concentration because of the current price of the material (\$400 per 740 g melt).

THEORETICAL BACKGROUND

Theory of Magnetic Cooling

The task of deriving a set of mathematical expressions which exactly describe a paramagnetic material when interactions are present is formidable. One usually makes simplifying assumptions which lead to approximate expressions which hopefully describe the system with sufficient accuracy. The following discussion is an attempt to describe the principle of the magnetic cooling process with simple mathematical expressions.

At sufficiently low temperatures only the ground state of a system of magnetic dipoles (electron spins) is occupied. If the ground state is characterized by a total angular momentum J , in units of \hbar , then, in the absence of any interactions, the ground state has a $(2J + 1)$ -fold degeneracy. In practice an interaction is always present, which causes at least a partial removal of the degeneracy or, equivalently, a splitting of the ground state energy level. One often assumes, for simplicity, that the ground state of each atom in zero external field is split up into $2J + 1$ equidistant levels of energy $E_m = mk\theta = -mg\beta h$, where $k\theta$ or $g\beta h$ is the energy separation between any two adjacent levels, k is Boltzmann's constant, g is the spectroscopic splitting factor, β is the Bohr magneton, and m takes on the $2J + 1$ values from $-J$ to $+J$. The quantities θ and h are then regarded as an interaction temperature and an effective internal magnetic field, respectively.

The partition function for a system of N magnetic atoms per unit volume in zero external field may be written as

$$Z_0 = \left(\sum_{m=-J}^J e^{-E_m/kT} \right)^N = \left(\sum_{m=-J}^J e^{mg\beta h/kT} \right)^N. \quad (1)$$

It is to be stressed that the use of an effective internal field h in the partition function to account for dipole-dipole interactions is an oversimplification. The ordering achieved in the dipole-dipole interaction is not completely equivalent to that obtained by applying an external field of magnitude h to a noninteracting system.

The quantity in parentheses can be expanded and grouped into two geometric series which can be summed. One then finds that

$$Z_0 = \left\{ \frac{\sinh [(2J + 1) X_0/T]}{\sinh (X_0/T)} \right\}^N, \quad (2)$$

where $X_0 = g\beta h/2k$.

The entropy and heat capacity of the system in zero external field are given by

$$S_0 = k \frac{\partial}{\partial T} (T \ln Z_0) \quad (3)$$

and

$$C_0 = T \frac{\partial S_0}{\partial T} . \quad (4)$$

It is assumed that the system has no P-V dependence; therefore, these variables are suppressed in the equations. Combining Eqs. (2) and (3), and then using Eq. (4), one obtains (e.g., see Sachs (5))

$$S_0 = Nk \left(\ln \frac{\sinh [(2J+1)X_0/T]}{\sinh X_0/T} - \frac{X_0}{T} \{ (2J+1) \coth [(2J+1)X_0/T] - \coth X_0/T \} \right) \quad (5)$$

and

$$C_0 = Nk(X_0/T)^2 \{ \operatorname{csch}^2 X_0/T - (2J+1)^2 \operatorname{csch}^2 [(2J+1)X_0/T] \} . \quad (6)$$

When the magnetic system is subjected to an external magnetic field of magnitude H the expressions for the partition function, entropy, and heat capacity have the same form as before but with X_0 replaced by X' , where

$$X' = g\beta H' / 2k \quad (7)$$

in which

$$H' = F(H, h) . \quad (8)$$

The functional form that should be used in Eq. (8) is not well understood; although, if $H \gg h$, one usually assumes $F(H, h)$ is approximately equal to H . The lattice entropy is usually negligible at and below 1°K and is, therefore, neglected.

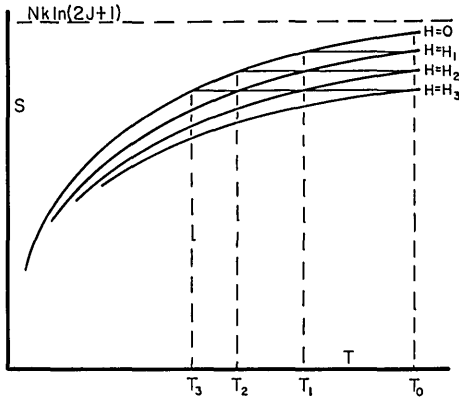


Fig. 1 - Entropy-temperature curves for a paramagnetic material

Figure 1 shows qualitative entropy-temperature curves for different magnetic field strengths. This figure demonstrates that an isothermal magnetization followed by an adiabatic or isentropic demagnetization will produce a cooling.

Following Kurti and Simon (6), the temperature reached immediately after demagnetization can be predicted approximately, provided that

$$T_i \gg g\beta h/k$$

and (9)

$$H_i \gg h ,$$

the inequality. The entropy change for the isentropic demagnetization to a field H_f is zero. Therefore,

$$S(H_i/T_i) = S(H_f/T_f) , \quad (10)$$

where T_f is the final temperature produced. Since the functional forms of the indicated

entropy equations are identical, the arguments of the functions must be equal in magnitude. Therefore,

$$H_i/T_i = H_f/T_f \tag{11}$$

or

$$T_f = H_f T_i / H_i .$$

On this model the final temperature reached is proportional to the initial temperature and the final field and is inversely proportional to the initial magnetizing field. A plot of T_f against various T_i/H_i values for constant H_f will yield a straight line with zero intercept.

Most demagnetizations are carried out to zero external magnetic field to prevent complications in susceptibility (and hence temperature) measurements. In this case one replaces H_f by the effective internal field h obtaining

$$T_f = h T_i / H_i , \tag{12}$$

but here the equality is on less certain footing. In practice, a plot of T_f versus T_i/H_i may or may not have the zero intercept predicted by Eq. (12).

The physical processes responsible for temperature reduction after adiabatic demagnetization can also be described in terms of energy level distributions (Fig. 2). Recall that, in the absence of external fields, the ground state energy level is assumed to be split into $2J + 1$ equidistant energy levels each separated by an energy $k\theta = g\beta h$. Each level corresponds to one of the $2J + 1$ orientations of the vector J . In the liquid helium range of temperature, $kT \gg k\theta$ for magnetically dilute paramagnetic materials. At these "high" temperatures, any of the $2J + 1$ orientations are equally probable; hence, the

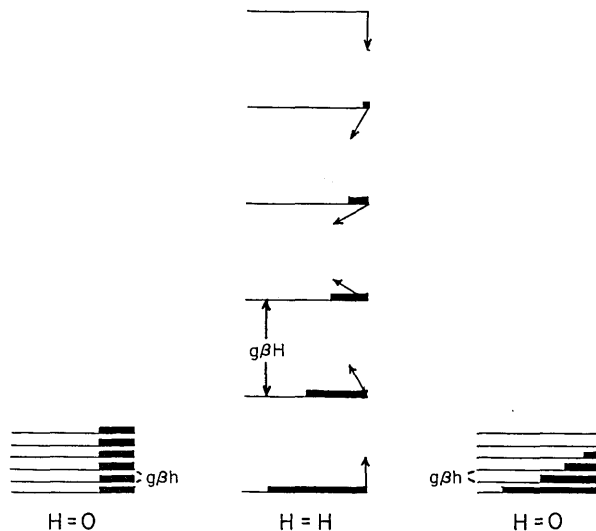


Fig. 2 - Energy level diagram for a paramagnetic system with $J = 5/2$ before magnetization, during magnetization, during magnetization, and after isentropic demagnetization. (After N. Kurti, in "Low Temperature Physics, Four Lectures," London: Pergamon Press, 1952, p. 30).

population of all levels is the same, as is indicated by the length of the horizontal "bars" superimposed on the energy levels. When a magnetic field H is applied such that $g\beta H \gg kT$, the splitting between adjacent levels ($g\beta\hbar$) is now much greater and the atoms go into the lower energy levels corresponding to dipoles pointing in the direction of the field. On removing the external field isentropically, the degree of order, and hence the population of the levels, must remain constant, but the splitting of the levels returns to the former value. It is obvious that to have such a "bottom-heavy" occupancy of the levels the temperature must have been lowered from the value prior to magnetization.

Low Temperature Paramagnetism

A material is said to be paramagnetic at a given temperature when its magnetic susceptibility χ is greater than zero and when there is no spontaneous ordering of the atomic magnetic moments. In general, electronic paramagnetism is found in all atoms and molecules having an odd number of electrons, since the total spin of such a system cannot be zero, and in all free atoms and ions with a partly filled inner shell. Frequently, but not invariably, these ions continue to exhibit paramagnetism when in solution and crystalline form. Paramagnetism is attributed to the incompletely filled 3d shell in the iron group and to the incompletely filled 4f shell in the rare-earth group.

Ideal Paramagnetism — An ideal paramagnetic material can be thought of as a system of N completely free magnetic dipoles per unit volume, each with a magnetic moment μ . In the classical theory of Langevin the magnetization produced by the alignment of the dipoles by an external field H is hindered by the thermal energy kT . The magnetization is given by

$$M = N\mu \left(\coth \frac{\mu H}{kT} - \frac{kT}{\mu H} \right). \quad (13)$$

In the limit when $\mu H/kT \ll 1$ the susceptibility is given by

$$\chi = M/H = N\mu^2/3kT = \lambda/T, \quad (14)$$

where λ is the Curie constant, equal to $N\mu^2/3k$.

A more sophisticated treatment considers the energy level structure of free atoms in a field H with total angular momentum J and z -component of magnetic moment $mg\beta$. The $2J+1$ degeneracy of the ground state energy level is completely removed upon application of an external field H . The additional energy of a level in the field H is known as the Zeeman energy and takes on the $2J+1$ values of J from $-J$ to $+J$. The partition function for this system is

$$Z = \left[\sum_{m=-J}^J e^{mg\beta\hbar/kT} \right]^N, \quad (15)$$

or

$$Z = \left\{ \frac{\sinh [(2J+1)g\beta H/2kT]}{\sinh (g\beta H/2kT)} \right\}^N. \quad (16)$$

The corresponding entropy and heat capacity expressions are identical to those given in Eqs. (5) and (6), respectively, with X_0 replaced by $X = g\beta H/2k$. The magnetization is given by

$$m = kT \frac{\partial}{\partial H} (\ln Z)$$

or

$$m = NJg\beta B_J(X),$$

(17)

where $B_J(X)$ is the well-known Brillouin function

$$B_J(X) = \frac{2J+1}{2J} \coth \left[(2J+1) \frac{X}{T} \right] - \frac{1}{2J} \coth \left(\frac{X}{T} \right).$$

(18)

In the limit when $g\beta H \ll kT$ the magnetization is given by

$$m = NJ(J+1)g^2\beta^2/3kT.$$

(19)

The corresponding magnetic susceptibility is

$$\chi = m/H = \lambda/T,$$

(20)

where the Curie constant λ is

$$\lambda = NJ(J+1)g^2\beta^2/3k.$$

(21)

Comparing Eqs. (20) and (21) to Eq. (14), the magnitude of the effective dipole moment is found to be

$$\mu = g\beta \sqrt{J(J+1)}.$$

(22)

In the special case where $J = 1/2$, the Brillouin function and entropy are given by

$$B_{1/2}(X) = \tanh (X/T)$$

(23)

and

$$S = Nk [\ln 2 + \ln \cosh (X/T) - (X/T) \tanh (X/T)].$$

(24)

Paramagnetism With Interactions — In practice one usually deals with atoms incorporated into solids and solutions instead of with the free atom. The effects of electric and magnetic interactions must be included in any detailed description of real paramagnetic materials. The interactions which may be present are the Stark interaction, the dipole-dipole interaction, hyperfine interactions, and exchange interactions.

1. Stark interaction: The surrounding magnetic and nonmagnetic atoms produce an inhomogeneous electric field at the site of each magnetic ion, resulting in the partial or complete removal of the degeneracy. This phenomenon is often referred to as the crystalline Stark effect or Stark splitting. According to Kramers' theorem,* when the angular-momentum quantum number of the system is a half integer there must always remain at least a twofold degeneracy associated with the two oppositely oriented components $\pm J_z$. Bethe (7) has shown that, from a knowledge of the symmetry of the crystalline field, the number and multiplicities of the new set of energy levels can be predicted. The arrangement of the levels and the magnitude of the splittings, however, cannot be predicted without detailed knowledge of the crystalline potential. This potential acts only upon the orbital part of the angular momentum, but it influences the spins through the spin-orbit interaction.

*See M. Sachs, "Solid State Theory," New York:McGraw-Hill, 1963, Appendix A.

When the crystal-field splitting is large and the lowest level is an orbital singlet, this level is nonmagnetic with respect to the orbits, and only spin-magnetism remains. This phenomenon is frequently referred to as orbital quenching.

In most materials used in magnetic cooling the effects on the susceptibility and heat capacity of dipole-dipole interactions are relatively weak at high temperature compared to those of Stark interactions.

The usual form of the partition function for Stark splitting is (8)

$$Z = \left(\sum_i 2n_i e^{-a_i k\delta/T} \right)^N, \quad (25)$$

where n_i is the number of Kramers' doublets at energy $a_i k\delta$, $k\delta$ is the overall splitting, and $0 \leq a_i \leq 1$. The splitting contributes a Schottky anomaly to the heat capacity ($C \propto T^{-2}$ at high temperatures).

Figures 3 and 4 show the effects of Stark and Zeeman splittings on the ground state levels of Cr^{3+} and Ce^{3+} , respectively. It is apparent that, for temperatures around 1°K , Stark splitting is important for Cr^{3+} while it is not important for Ce^{3+} provided the crystalline fields possess, at most, hexagonal symmetry.

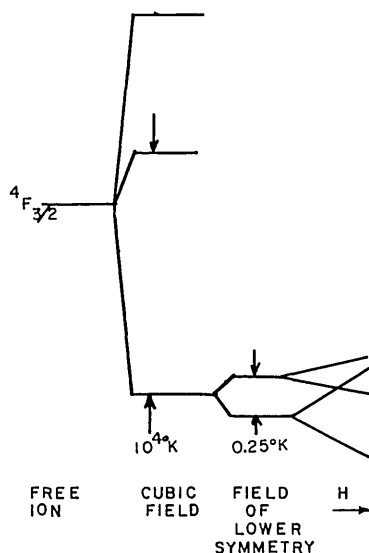


Fig. 3 - Stark and Zeeman splitting of the ground state energy level for Cr^{3+} (not to scale). [After A. D. Pickar, NBS Report 7529, 7, 1962].

2. Dipole-dipole interaction: The magnitude of the dipole-dipole interaction is governed mainly by the magnitude of the dipole moments and their average separation. A rigorous mathematical description of the problem necessitates the solution of a many-body problem; nevertheless, one can estimate the order of magnitude of the critical temperature T_c at which interactions between two dipoles become appreciable. If the moment of each dipole is 1 Bohr magneton, then the order of magnitude of T_c is given by $\beta^2/a^3 = kT_c$, where a is the average distance between dipoles. For cerium magnesium nitrate, a better approximation is

$$5.6\beta^2/a^3 = kT_c. \quad (26)$$

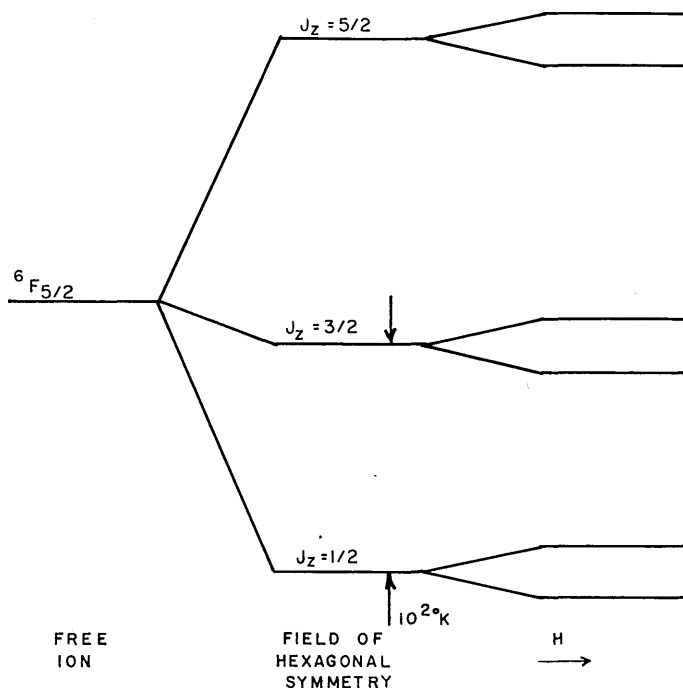


Fig. 4 - Stark and Zeeman splitting of the ground state energy level for Ce^{3+} . The order and magnitude of the level spacings are arbitrarily assigned. [After M. Sachs, "Solid State Theory," New York:McGraw-Hill, 1963, p. 116].

The effect of the interaction is to split each energy level into a band of levels of separation $g\beta h$ or $k\theta$, where h is the rms internal field due to the surrounding dipoles, and θ is an interaction temperature.

The approximate zero field partition function, entropy, and heat capacity functions have been given in Eqs. (2), (5), and (6), respectively. The heat capacity goes through a maximum in the region $X_0/T \sim 1$. For $J = 1/2$ Eq. (6) becomes

$$C_0/Nk = (X/T)^2 \operatorname{sech}^2(X/T), \quad (27)$$

which has a maximum at $X/T = 1.2$ or $T = \theta/2.4$. A curve of C_0 versus T/X for $J = 1/2$ is shown in Fig. 5. The large bump in the heat capacity is due to the comparatively large thermal energy required to excite transitions to states of higher energy when T becomes of the order of θ .

When $T \gg \theta$, Eq. (6) simplifies to

$$C_0 = NRJ(J+1)\theta^2/3T^2 = \lambda h^2/T^2. \quad (28)$$

Hence, at high temperatures the heat capacity increases as the reciprocal temperature squared.

The dipole-dipole interaction can have either a ferromagnetic or an antiferromagnetic effect on the susceptibility.

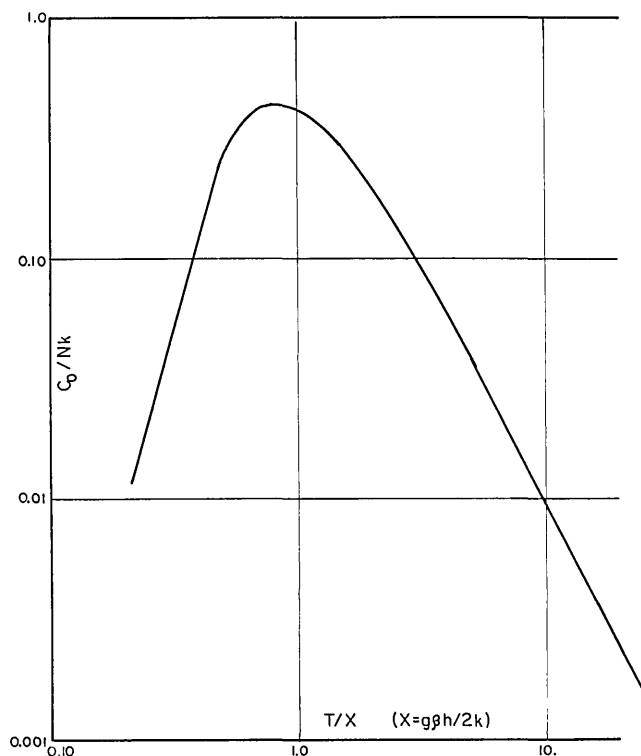


Fig. 5 - Temperature dependence of the heat capacity of a paramagnetic material with $J = 1/2$

3. Hyperfine interactions: Two kinds of hyperfine interactions are usually considered. One of these may occur if the nucleus of the paramagnetic ion has a nuclear moment which interacts with the electronic magnetic moments of the ion.

The second kind of hyperfine interaction which may occur is due to the interaction of the electric quadrupole moment of the nucleus with the gradient of the crystalline electric field at the nucleus.

The hyperfine interactions contribute a T^{-2} term to the heat capacity but do not have a significant effect on the susceptibility.* Since Ce^{140} has neither a nuclear spin nor an electric quadrupole moment, no hyperfine interactions are expected in cerium compounds.

4. Exchange interactions: The exchange interaction is strictly quantum mechanical in nature, arising, as a consequence, from the application of the Pauli exclusion principle to the Coulomb interactions between electrons. In the magnetically dilute materials used in magnetic cooling, exchange effects are often assumed to be negligible because of the large distances separating magnetic ions.

*See A. H. Cooke, "Progress in Low Temperature Physics," Amsterdam:North-Holland, 1957, Vol. 1, p. 230.

Suitable Cooling Materials

Requirements — In order that a paramagnetic material be suitable for producing low temperatures upon adiabatic demagnetization, it must possess a nontrivial amount of entropy which is almost completely removable by magnetic fields of accessible magnitude. To judge whether a given material is suitable requires a knowledge of the separations of the low-lying energy levels, or at least an assurance that the temperature corresponding to the intrinsic magnetic interaction is at least an order of magnitude lower than the temperature at which the isothermal magnetization is carried out. In addition, one requires the material to have sufficient heat capacity at low temperatures to combat the unavoidable heat leak into the heretofore assumed "adiabatic" chamber of the apparatus.

Materials in Current Use — A list of some paramagnetic materials commonly used in magnetic cooling is given by Hoare, Jackson, and Kurti (9). This list is given in Table 1 together with an indication of the lowest temperature obtainable.

Paramagnetic metals (10) have recently been used for adiabatic demagnetization, but, so far, the lowest temperature produced with these materials has been 0.09°K .

EXPERIMENTAL BACKGROUND

Temperature Measurement

Ballistic Susceptibility Bridge — The most common method of temperature measurement in adiabatic demagnetization work is the measurement of the magnetic susceptibility, which is related to the absolute temperature by Curie's law, $\chi \propto 1/T$. A ballistic-galvanometer circuit is frequently used to measure the susceptibility. A typical circuit is shown in Fig. 6. The circuit is essentially a transformer. The primary coils P and P' are driven with current I by a battery, and the current can be pulsed from I to $-I$ by throwing the reversing switch R . The secondary is terminated with the ballistic galvanometer G which responds to the signal induced in the secondary upon reversal of current in the primary. The secondary coils $S1$ and $S2$ (usually several thousand turns each) are wound in opposition such that, in the absence of a magnetic specimen (shown in coil $S1$), no signal is induced in the secondary upon reversal of I . The external nulling variable mutual inductor M_v is used as a fine adjustment trimmer in signal nulling by the opposing $S1$ and $S2$ coils. The net mutual inductance between primary and secondary circuits is essentially zero until a magnetic specimen is introduced into secondary $S1$. Then, due to the distortion of the flux lines, a finite mutual inductance exists between the two circuits.

The magnitude of the ballistic deflection of the galvanometer upon reversal of I is given by

$$\delta = K' M \Delta I / R, \quad (29)$$

where K' is a galvanometer constant, M is the net mutual inductance between circuits, and R is the total secondary resistance. For the special case where the coils are cylindrical and coaxial, P is infinitely long, the center of $S1$ coincides with the center of the prolate spheroidal specimen, and $S2$ is far enough from the specimen such that the flux lines are again uniform, an exact expression can be obtained for M from the work of

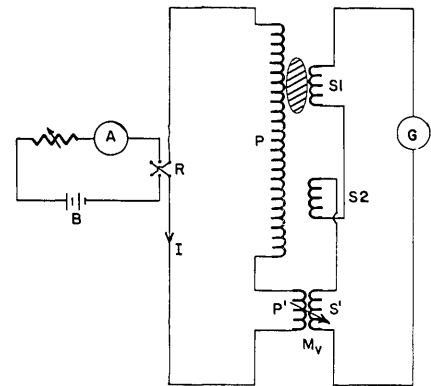


Fig. 6 - Typical ballistic galvanometer circuit

Spohr and Althouse (unpublished) and, with some ingenuity, from the work of Pal, Tarnoczi, and Nemeth (11). The expression is

$$M = BM_0\chi_X = \frac{BM_0f\lambda}{T - f\lambda(4\pi/3 - N)} \quad (30)$$

Here B is a complicated geometric factor with three independent variables, M_0 is the mutual inductance between P and S_1 with no specimen present, χ_X is the susceptibility calculated by dividing the magnetization by the external field that would be present in the absence of a specimen, f is a filling factor which accounts for the deviation from crystalline density for powdered specimens, and N is the demagnetization factor. The last equality in Eq. (30) assumes the validity of Curie's law.

Equation (29) now becomes

$$\delta = K\Delta I / (T - \underline{\Delta}), \quad \underline{\Delta} = f\lambda(4\pi/3 - N) \quad (31)$$

where K is a constant of the apparatus and is determined by calibration. The shape correction factor $\underline{\Delta}$ will be discussed later.

The system is calibrated in the liquid helium range of temperatures (1 to 4.2°K) by allowing the specimen to come into thermal equilibrium with the liquid helium bath, reversing the primary current, and observing the galvanometer deflection. A curve of δ versus $(T - \underline{\Delta})^{-1}$ is plotted, and the constant K is found from the slope. This curve is referred to as the Curie plot.

The temperatures attained after demagnetization are determined by taking more galvanometer readings and using the calibration determined at higher temperatures. As long as the susceptibility obeys Curie's law, the temperature calculated from the galvanometer deflection is identical to the absolute temperature. At low temperatures deviations from Curie's law occur sooner or later, and for this reason one replaces T by T° (magnetic temperature) in Eq. (30). Some independent experiment must then be carried out to correlate T and T° .

Origin of the Shape Correction Factor — The discussion given here elaborates on that given by White (12) and is limited to the special case of spheroidal specimens. The following magnetic fields and susceptibilities are defined for convenience:

H_0 is the uniform magnetic field that existed in the absence of the specimen.

H_I is the uniform macroscopic field inside the specimen.

$$H_I = H_0 - Nm.$$

H_L is the microscopic field at the site of an atom.

$$H_L = H_0 + [(4\pi/3) - N]m, \text{ which is the Lorentz local field approximation in which the contribution of the dipoles inside the Lorentz cavity is zero.}$$

$$\chi_X = m/H_0.$$

$$\chi_L = m/H_L.$$

The shape factor arises from the interpretation that it is the local susceptibility which actually obeys Curie's law. Equations (29) and (30) show that the galvanometer deflection depends on χ_X ; therefore, one solves for χ_X in terms of χ_L with the subsequent substitution of $\chi_L = f\lambda/T^{\circ}$. One readily obtains

$$\chi_X = \frac{\chi_L}{1 - [(4\pi/3) - N]\chi_L} = \frac{f\lambda}{T^{\otimes} - \Delta} \quad (32)$$

For a spherical specimen N is $4\pi/3$ so that the shape factor Δ vanishes.

Shape Factors for Cylinders — Because of the ease of preparation, one usually uses cylindrical rather than spheroidal specimens. Unfortunately, the demagnetization factor of a cylindrical specimen is a function of position as well as of the magnitude of the susceptibility. In the limiting case for $\chi \rightarrow 0$, Joseph (13) has calculated two average demagnetization factors — the so-called ballistic and magnetometric demagnetization factors. One can usually take a weighted average of these two factors appropriate to the apparatus when calculating an average demagnetization factor to be used in determining the shape correction factor Δ .

T^{\otimes} - T Correlation — A simple method of observing deviation from Curie-law behavior is to embed one end of a system of copper wires into the paramagnetic material under investigation and the other end into a low-heat-capacity paramagnetic material (thermometer) having an established temperature scale (see Fig. 7). The unknown material is demagnetized and the thermometer is cooled with it. The susceptibilities of the two materials are measured simultaneously and correction factors are obtained for the magnetic temperature scale. A temperature-dependent thermal gradient may exist between the unknown and the thermometer due to the finite heat capacity of the thermometer, the temperature-dependent thermal conductivity of copper, and the temperature-dependent thermal impedance of the boundary layer between the paramagnetic materials and the copper wires. This gradient is calculable and should be negligible above 0.050°K for a heat leak of 50 erg/min into the thermometer of the system designed.

Thermal Contact at Low Temperatures

Since paramagnetic materials are frequently used to cool other materials below 1°K via a copper wire or fin heat link, and since the coolant material is also used as a thermometer for the entire system, the establishment of thermal equilibrium is of utmost importance.

Thermal Conductivity of Copper Wire — Nicol and Tseng (14) have measured the thermal conductivity of General Electric commercial high-purity polycrystalline copper wire from 0.25 to 4.2°K . The trend of their data at the lowest temperatures is toward a temperature-dependent thermal conductivity given by $K(T) = 1.3 T \text{ W/cm}^\circ\text{K}^2$.

Consider a copper rod of cross-sectional area A and length L having a constant heat leak of \dot{Q} into one end while the other end is maintained at constant temperature T_k . The temperature difference ΔT across the rod can be calculated from the thermal conductivity equation

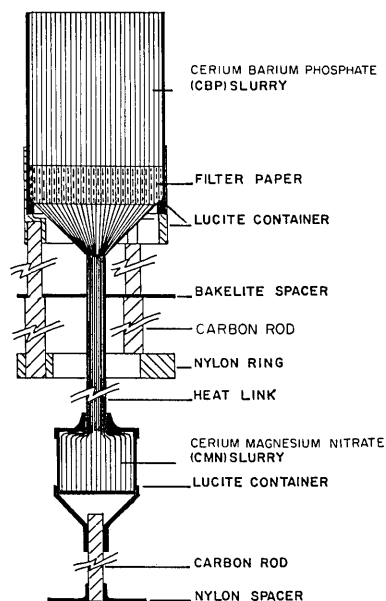


Fig. 7 - Specimen assembly with carbon rod supports used in the T^{\otimes} - T correlation experiments

$$\dot{Q} = \frac{A}{L} \int_{T_k}^{T_H} K(T) dT = 0.65 \frac{A}{L} [T_H^2 - T_k^2] , \quad (33)$$

where T_H is the temperature at the other end of the rod. One can show that $\Delta T \approx 0.0006^\circ\text{K}$ at $T_k = 0.01^\circ\text{K}$ for a heat leak of 50 erg/min into a wire bundle with dimensions $A = 0.20 \text{ cm}^2$ and $L = 20 \text{ cm}$, which are representative of the experimental apparatus.

T^3 Law — The most serious problem in maintaining thermal equilibrium at low temperatures is in the thermal contact between the paramagnetic material and the copper wire or fin heat link. The temperature dependence of the thermal contact has been investigated by others* who found a relationship

$$\dot{Q} = \xi A (T_H^3 - T_c^3) , \quad (34)$$

where ξ is a constant of the order of $10^3 \text{ erg/cm}^2 \cdot ^\circ\text{K}^3 \cdot \text{sec}$. A is the surface area of contact, T_H and T_c are the temperatures of the hotter and colder medias, respectively, and \dot{Q} is the heat flow across the junction.

When there are two junctions, Eq. (34) can be rewritten as

$$\dot{Q} = \xi \frac{A_1 A_2}{A_1 + A_2} [T_H^3 - T_c^3] , \quad (35)$$

where A_1 and A_2 are the surface areas of contact of the two materials with the heat link.

An estimate of the seriousness of the contact resistance at $T_c = 0.01^\circ\text{K}$ with $\dot{Q} = 50 \text{ erg/min}$ can now be calculated and compared with that due to the finite conductivity of copper. A value of $A_1 A_2 / (A_1 + A_2) = 150 \text{ cm}^2$ is appropriate for the experimental system to be used. One finds the temperature difference to be about 0.0087°K , which is significant. At $T_c = 0.05^\circ\text{K}$, however, ΔT has diminished to 0.0007°K .

Ce(PO₃)₃-Ba(PO₃)₂ GLASS

Known Properties

Faraday rotation experiments were conducted on CBP glasses by Alers (15) in 1959. Samples of 20-, 50-, 80-, and 100-wt-% cerous metaphosphate were investigated at 4.2°K and 1.8°K . The experiments indicated a J value of $1/2$ and a spectroscopic splitting factor g of 1.75, which maintained a constant value over the range of compositions stated. The constancy of g , as well as the fact that the rotations at 4.2°K and 1.8°K fell on the same curve, suggested the absence of magnetic interactions in the liquid helium temperature range. The glass was purchased from the Bausch and Lomb Optical Company.

Faraday rotation was measured from 13°K to 337°K and magnetic susceptibility was measured from 1.4°K to 296°K on a sample of cerous metaphosphate by Berger and Rubinstein (16) in 1964. The glass had a very high cerium concentration, analysis indicating a composition $\text{Ce}_2\text{O}_3 \cdot 2.67 \text{ P}_2\text{O}_5$. Again the experiments indicated $J = 1/2$; however, this time g was temperature dependent ($g = 1.71$ at 1.4°K and 1.90 at 4.2°K). An experiment on a less concentrated cerous metaphosphate glass yielded a splitting factor of $g = 2$, which indicated composition dependence as well. The density of the $\text{Ce}_2\text{O}_3 \cdot 2.67 \text{ P}_2\text{O}_5$ glass was stated to be 3.54 gm/cm^3 . The glass was apparently prepared by coworkers.

*See Ref. 9, pp. 191-192.

Choice of 50% $\text{Ce}(\text{PO}_3)_3$ - $\text{Ba}(\text{PO}_3)_2$

With the properties reported above for the cerous glasses ($J = 1/2$, $1.7 \leq g \leq 2$), one can calculate approximately the expected Curie constant, dipole-dipole heat capacity, and the order of magnitude of the temperature corresponding to the dipole-dipole interaction for various cerous ion concentrations. For the composition 50-wt-% cerous metaphosphate, one calculates $\lambda = 0.0014$ volume cgs units, $\theta = 5.6 \beta^2/\text{ka}^3 = 0.011^\circ\text{K}$, and $C_0 = 3.5/T^2 \text{ erg}/^\circ\text{K cm}^3$. The interaction temperature of 0.011°K indicates that temperatures of the order of 10 millidegrees might be reached, and the calculated heat capacity is large enough to prevent rapid warmup after demagnetization, assuming heat leaks of 50 to 100 ergs/min. The Curie constant is intermediate between that for CMN (0.00057 for powdered sample) and CPA (0.0068), indicating that the sensitivity of normal susceptibility measurement systems should be adequate. The 50% composition was chosen for the experiments because of the reasonable values of the above parameters.

APPARATUS

Exchange Gas System

A schematic of the vacuum-tight chamber containing the specimen and thermometer is shown in Fig. 8. The entire system, including the two sets of susceptibility coils, are housed in a helium dewar in which the temperature can be lowered to 1.3°K by pumping away the vapor boiling from liquid helium. The walls of the container were made from 2-1/16-in.-O.D. and 1-5/16-in.-O.D. brass telescopic tubing. All the flanges were turned from brass, and all joints below the copper-twist radiation baffle were silver-soldered to eliminate superconducting loops. The gold o-ring seal, which facilitated specimen changes, was made by compressing a 0.025-in.-thick gold o-ring between brass flanges drawn together by sixteen 5-40 brass fillister-head screws.

A 1/2-W Speer carbon radio resistor (mixed No. 1002) was used to monitor the temperature of the specimen just before demagnetization, when there was no thermal contact with the bath. Number 40 A.W.G. manganin wires of about 24-in. lengths were run from the resistor to the solder terminals on the "pump line termination flange" to minimize heat leak into the specimen. The terminals were electrically connected to the outside by No. 36 A.W.G. copper wires which ran up the pumping line after being thermally shorted to bath temperature by 25 turns around the copper "thermal shorting spool." A multiple-connection glass-to-metal seal was used to lead the copper wires through at the top of the apparatus.

Helium exchange gas was admitted through the pumping line by a Circle Seal 9459B-2MM needle valve, and an air-cooled VMF 20 oil diffusion pump was used for evacuation.

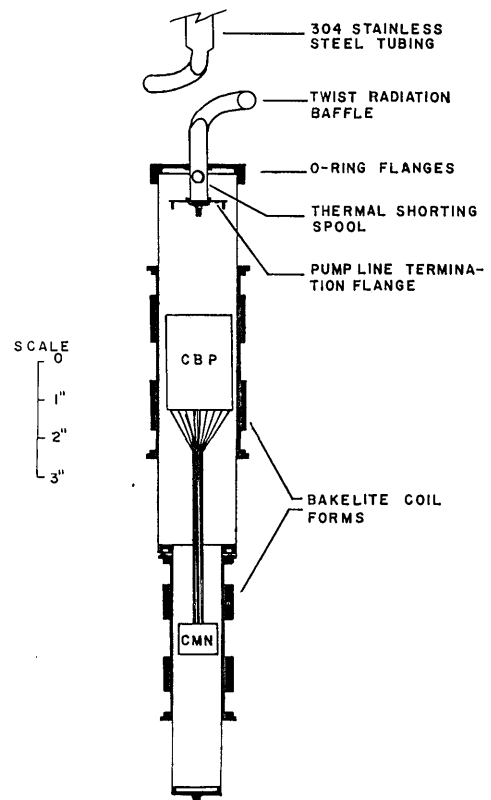


Fig. 8 - Vacuum can, specimen, and susceptibility coil assembly

Specimens

Slurry Preparation — In all experiments with the 50% CBP glass, the glass was first pulverized with a brass rod and container and was then ground with a mortar and pestle so that the powder passed through a sieve with 0.007-in. openings. A slurry was then prepared by mixing the powder with a solution of 60% glycerine, 35% distilled water, and 5% Aerosol O.T. wetting solution (25%).

For the T° - T correlation experiments the glass slurry was poured into a Lucite cylindrical shell of 1-3/4-in.-I.D. and 2-1/2-in. length into which 4306 No. 40 A.W.G. Formvar insulated copper wires had previously been uniformly distributed. The wires, which protruded approximately 8 in. from the bottom of the specimen, were tightly bundled together, resembling a solid rod of copper. The lower end of the rod was then frayed and inserted into a smaller Lucite cup of 1-in. I.D. and 13/16-in. length. A hypodermic needle was used to admit a similarly prepared slurry of CMN into the lower cup through a hole in its lid. The total copper wire surface area in the upper and lower specimens was 541 cm² and 203 cm², respectively.

Heat Link Fabrication — The method of preparation of the wire bundle to be embedded, reasonably uniformly, in the glass slurry was identical to that first devised and used by Spohr (17). A tubular mandrel of about 12-in. circumference and 18-in. length was mounted between the chuck and the tailstock of a metal lathe. Long strips of 1/2-in.-wide filter paper were lightly glued with rubber cement to the surface of the mandrel, parallel to the axis, at intervals calculated to give the spacing required in the subsequent procedure. Number 40 A.W.G. Formvar enameled copper wire was then wound onto the mandrel over the strips from a pulley assembly held in the lathe tool post with the longitudinal feed of the lathe engaged to give a spacing of 0.026 in. between adjacent wire centers.

After progressing laterally to the end of the mandrel, the winding operation was stopped, and the wires were glued to the strips with water-diluted Elmer's Glue-all. When the glue was dry, the wire and the paper were removed from the mandrel by cutting along an appropriate line parallel to the axis of the mandrel, and the resultant wire sheet was then flattened out. One then had about 600 wires of 12-in. length running parallel to each other at separations of 0.026 in., held firmly in place by strips of filter paper running perpendicular to the direction of the wires. The sheet was then rolled up tightly along an axis parallel to the direction of the wires until the diameter of the bundle was approximately 1-3/4 in. The wire bundle was then threaded through a 1/32-in.-wall Lucite cylinder with a slight constriction at one end until the appropriate filter paper strip was held firmly at the constriction.

For the other experiments no wire heat link was required; hence the slurry was simply poured into a cylindrical container.

Specimen Support — In the early experiments the CBP specimen assembly was held in a Lucite cup supported by three 3-1/2-in.-long Sr 50 Ultra Carbon rods which were held at the bottom in a nylon ring resting on the constriction in the exchange gas can. About halfway up the rods, where their diameter was reduced from 0.242 in. to 0.185 in., a three-point Bakelite ring spacer was situated such that the three points just touched the walls of the exchange can.

The use of graphite supports at low temperatures has been reported by Shore et al. (18). This method of support led to rather large heat leaks and was abandoned in the latter experiments in favor of hanging the CBP specimen from a cotton thread with four-point Bakelite spacers glued to the top and bottom of the Lucite specimen container. The CMN thermometer was held centrally in the exchange gas system by a four-point nylon spacer attached to its bottom by a 1-1/2-in.-long by 0.242-in.-O.D. carbon rod. A

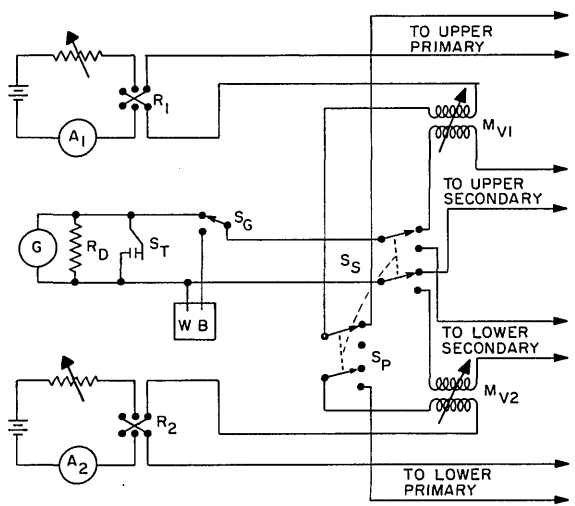
diagram of the specimen assembly with graphite supports used in the $T^{\circ}-T$ correlation experiments is shown in Fig. 7.

Susceptibility Measurement Circuit

A Leeds and Northrup ballistic galvanometer, model 2285A, was used for the susceptibility measurements. The galvanometer had a sensitivity of $0.08 \mu\text{V}/\text{mm}$, a critical damping resistance of 29 ohms, an internal resistance of 17 ohms, and a period of 9.0 sec. Two independent ballistic circuits, one for each susceptibility system, were connected to the galvanometer by means of the coupled switches S_s and S_p (Fig. 9).

The design of the Bakelite forms for the susceptibility coils is shown in Fig. 10. The innermost grooves were filled with the secondary windings, and then the remaining outermost groove was filled with primary windings. Extra turns were put on the ends of the primary coils to provide a more nearly uniform field in the vicinity of the center of the coil where the specimen was located. As described in the temperature measurement section, the secondary always consists of two oppositely wound sections. Figure 10 shows that the opposing secondary was split in half with each half placed near the end of the coil form. This arrangement allowed the specimen to be centered inside the coil system.

The upper coil system, used for measurements on the CBP glass slurry, had 4344 turns of No. 40 A.W.G. copper wire in the central secondary and 1810 turns of No. 32 A.W.G. copper wire in the primary. The lower coil system, used for measurements on the CMN thermometer, had 15,294 turns of No. 42 A.W.G. copper wire in the central secondary and 2488 turns of No. 30 A.W.G. copper wire in the primary.



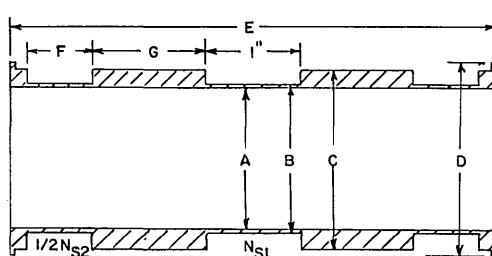
S_s & S_p : COUPLED SWITCHES TO SELECT EITHER UPPER OR LOWER COIL SYSTEM

WB: WHEATSTONE BRIDGE

S_g : SELECTOR SWITCH FOR GALVANOMETRIC OR RESISTIVE MEASUREMENTS

S_T : GALVANOMETER SHORTING SWITCH

R_D : GALVANOMETER DAMPING RESISTOR



UPPER COIL FORM

A = 2.072"	$N_{S1} = 4,344$ TURNS
B = 2.141"	
C = 2.511"	$N_{S2} = 5,728$ TURNS
D = 2.607"	
E = 5.125"	$N_p = 1,810$ TURNS
F = 0.685"	
G = 1.188"	

LOWER COIL FORM

A = 1.320"	$N_{S1} = 15,294$ TURNS
B = 1.380"	
C = 1.817"	$N_{S2} = 15,276$ TURNS
D = 2.000"	
E = 4.125"	$N_p = 2,488$ TURNS
F = 0.645"	
G = 0.729"	

Fig. 9 - Ballistic susceptibility measurement circuit used in the experiments

Fig. 10 - Design of the Bakelite susceptibility coil forms

The Dewar

The dewar used in the experiments consisted of a nested metal nitrogen dewar and glass helium dewar. The minimum I.D. of the helium dewar was 3.54 in., and the maximum O.D. of the tail section of the nitrogen dewar was slightly less than 4.25 in. The dewar was borrowed from R. A. Hein of the Naval Research Laboratory.

The Magnet

The magnet used was the 4.25-in.-I.D. Bitter-type water-cooled solenoid in the high-field magnet facility of the Naval Research Laboratory. The 3.2 MW of available power will energize this magnet to a field of about 90 kG.

EXPERIMENTAL PROCEDURE

Density Measurement

The density of a 7.8-g piece of 50% CBP glass was measured on an analytical balance by weighing the suspended piece in air and in distilled water. The density was computed from the formula $d = m_A / (m_A - m_W)$, where m_A is the mass in air, and m_W is the mass in water.

Specimen Analysis

Several grams of the powdered CBP glass were given to O. R. Gates of the Naval Research Laboratory, who performed a volumetric or titration analysis to determine the actual Ce^{3+} concentration.

Curie Constant Measurement

A 1/32-in.-wall Lucite cylindrical container of 1.75-in. I.D. and 2.5-in. length was rigidly held in place inside the apparatus. The container was filled with a slurry containing a known amount of CPA, and a Curie plot was taken in the range 4.2°K to 1.3°K. The container was then refilled with a slurry containing a known amount of 50% CBP glass powder, and another Curie plot was taken. From the slopes of the two curves, the known filling factors, and the known Curie constant of CPA, the Curie constant was determined for the glass. The maximum field used in any of the susceptibility measurements in the liquid helium temperature range was 50 Oe.

Adiabatic Demagnetization

The apparatus was precooled overnight to 77°K by thermal conduction to the liquid nitrogen bath through nitrogen gas of about 1 atm pressure inside the helium dewar and helium dewar vacuum space. When the apparatus reached 77°K, the helium dewar vacuum space was evacuated to about 30 μ pressure and sealed off by turning a glass stopcock. The exchange gas can was evacuated to about 0.1 μ and then filled with helium gas at 1 to 5 μ pressure through the needle valve in the pumping line. The dewar was evacuated, filled with 1 atm of helium gas, and then filled with about 10 l of liquid helium from a transport dewar.

While maintaining 1 to 5 μ exchange gas pressure, two size 8-8-10 Kinney mechanical pumps, in parallel, were used to pump the helium bath from 4.2°K to 1.3°K, stopping

at various temperatures to take galvanometer and carbon resistor-thermometer readings. A Texas Instruments Inc. fused-quartz precision pressure gauge, model 141A, was used to measure the helium vapor pressure. The absolute temperature was determined from the 1958 He⁴ vapor pressure tables. A borrowed, homemade dc Wheatstone bridge, operating at 20 mV, was used for the carbon resistor measurements. For future reference, the galvanometer deflections and carbon resistor readings were plotted against $1/T$.

At about 1.3°K the system was magnetized. Since the system was usually magnetized too rapidly to maintain isothermal conditions, the carbon resistor, in thermal contact with the specimen, was monitored. When the resistance corresponding to 1.3°K was regained, the heat of magnetization was removed. The exchange gas can was then evacuated to about 0.01 μ pressure, followed by the demagnetization at a rate of about 12.5 kG/min.

When the demagnetization was completed, galvanometer deflections and elapsed time were recorded, taking four readings in rapid sequence for each system. At the end of the experiment the galvanometer deflections were plotted as a function of time and a smooth curve was drawn through the data. The agreement between the indicated specimen and the thermometer temperatures was obtained at a given time by reference to these curves and the Curie plots.

In later $T^{\circ}-T$ experiments the dewar was lifted out of the magnet and suspended from the hoist with nylon ropes before any measurements were made. This resulted in a longer warmup time, attributed to smaller vibrational heating.

For a given demagnetization, the value of H/T_i was determined from the magnet current and field constant and from the value of the carbon resistor prior to demagnetization.

EXPERIMENTAL RESULTS

Density

The density of the 50% CBP glass was 3.57.

Specimen Analysis

The volumetric analysis indicated a Ce³⁺ concentration of 16.1% by weight, which is 8.7% higher than that expected for the 50% CBP glass. This corresponds to $N = 3.11 \times 10^{21}$ Ce³⁺ ions/cm³, which gives an average cerium ion separation of $N^{-1/3} = 6.85 \times 10^{-8}$ cm.

Curie Constant

The Curie constant was found to be within the limits $0.00189 \leq \lambda \leq 0.00224$ volume cgs units.

Temperatures Produced from Different H/T 's

Figures 11 and 12 are graphs of the magnetic temperatures T° produced from the various H/T_i and T_i/H values, respectively. The magnetic field was not corrected for demagnetization effects, which amount to about 14% at 0.05°K. Superimposed on Figs. 11 and 12 are the equivalent curves for CPA and CMN, as determined by other workers in

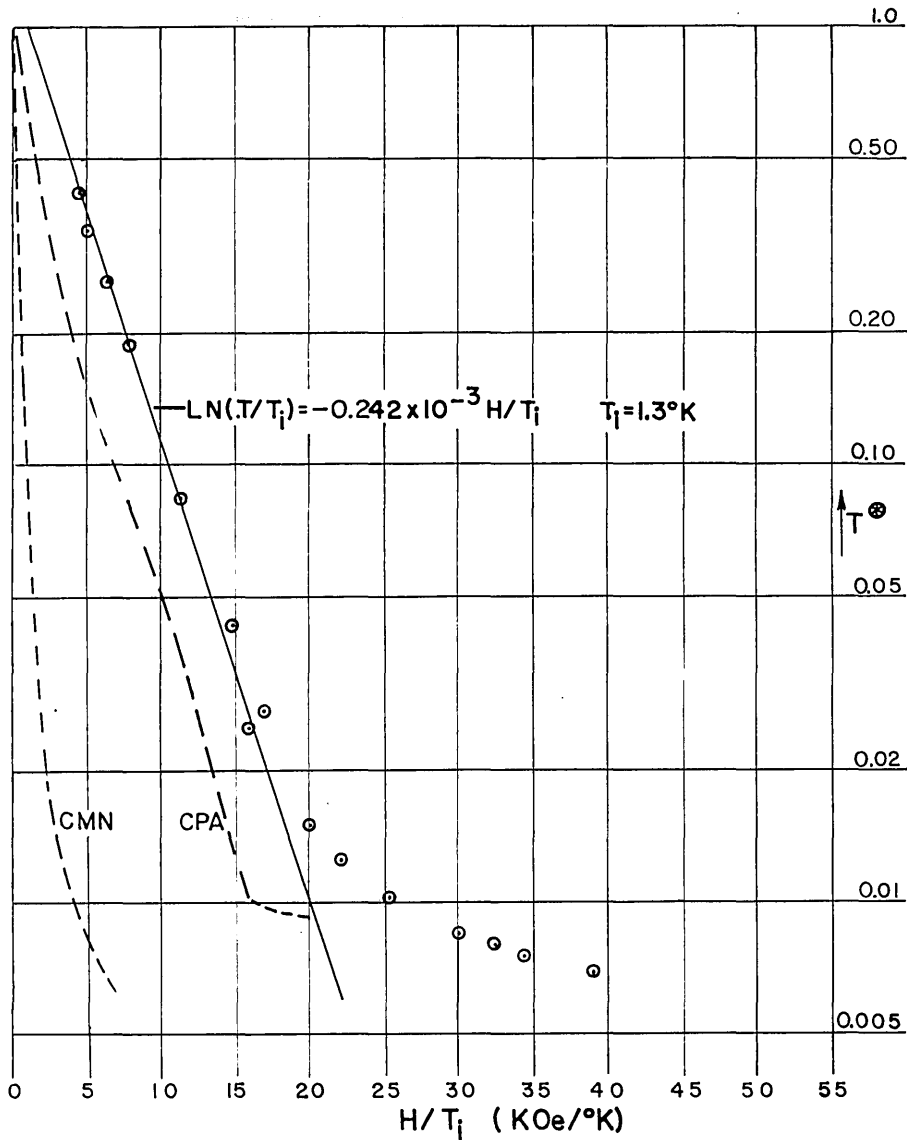


Fig. 11 - Magnetic temperatures produced as a function of H/T . Absolute, rather than magnetic, temperatures are used for CMN and CPA.

the field. The CMN data were taken from Ref. 1, and the CPA data represent an average of the data in Refs. 20 and 21. The experimental data for the glass is presented in Table 2.

T^{\otimes} - T Correlation

Figures 13 through 19 show the percentage deviation of the temperature of the CMN thermometer from the magnetic temperature of the CBP glass for various experimental runs. Because of the expected thermal contact problems mentioned earlier, no graphical data are presented below 0.05°K . A portion of the correlation data for run VIII is presented in Table 3.

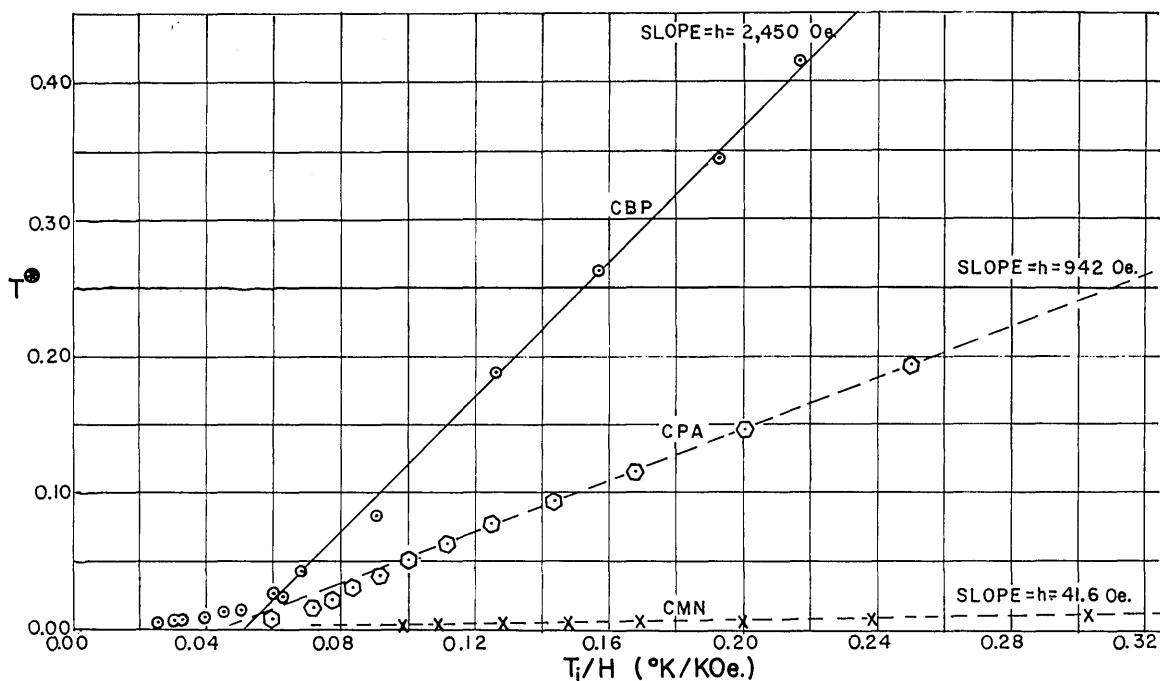


Fig. 12 - Magnetic temperatures produced as a function of T_i/H . Absolute, rather than magnetic, temperatures are used for CMN and CPA.

Table 2
Magnetic Temperatures Produced From Various H/T Values

H (kG)	$1/T$ ($^{\circ}\text{K}^{-1}$)	H/T (kG/ $^{\circ}\text{K}$)	T_i° ($^{\circ}\text{K}$)	Cylinder Diameter (in.)	Cylinder Length (in.)	Average Demag- netization Factor	f	Δ ($^{\circ}\text{K}$)
5.88	0.783	4.60	0.416	1.69	2.44	2.21	0.533	0.00201
6.62	0.783	5.18	0.344	1.69	2.44	2.21	0.533	0.00201
8.09	0.785	6.35	0.263	1.69	2.44	2.21	0.533	0.00201
10.1	0.786	7.91	0.189	1.69	2.44	2.21	0.533	0.00201
14.9	0.756	11.3	0.0841	1.69	2.44	2.21	0.533	0.00201
18.6	0.787	14.7	0.0428	1.69	2.44	2.21	0.533	0.00201
22.4	0.753	16.9	0.0275	1.69	2.44	2.21	0.533	0.00201
19.6	0.818	16.0	0.0251	1.44	1.44	3.62	0.55	0.00062
24.9	0.803	20.0	0.0150	1.44	1.44	3.62	0.55	0.00062
27.5	0.802	22.1	0.0125	1.44	1.44	3.62	0.55	0.00062
31.6	0.805	25.4	0.0102	1.44	1.44	3.62	0.55	0.00062
37.2	0.805	29.9	0.00845	1.44	1.44	3.62	0.55	0.00062
39.9	0.810	32.3	0.00802	1.44	1.44	3.62	0.55	0.00062
42.6	0.804	34.2	0.00746	1.44	1.44	3.62	0.55	0.00062
48.0	0.810	38.9	0.00694	1.44	1.44	3.62	0.55	0.00062

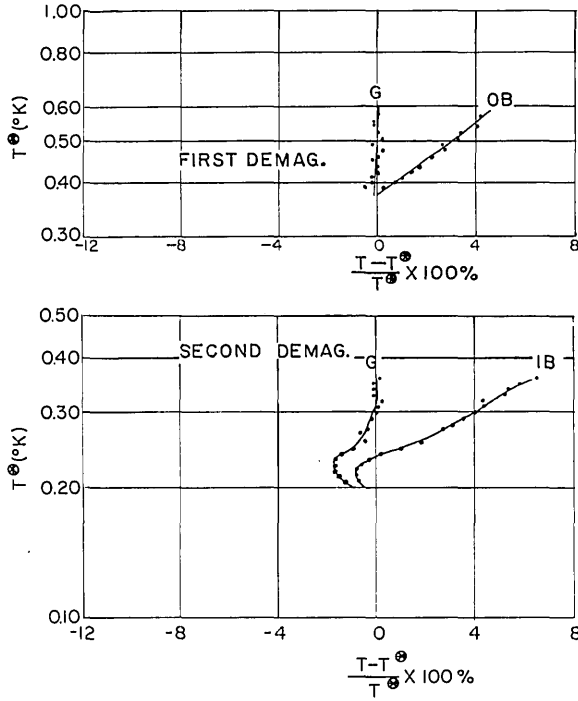
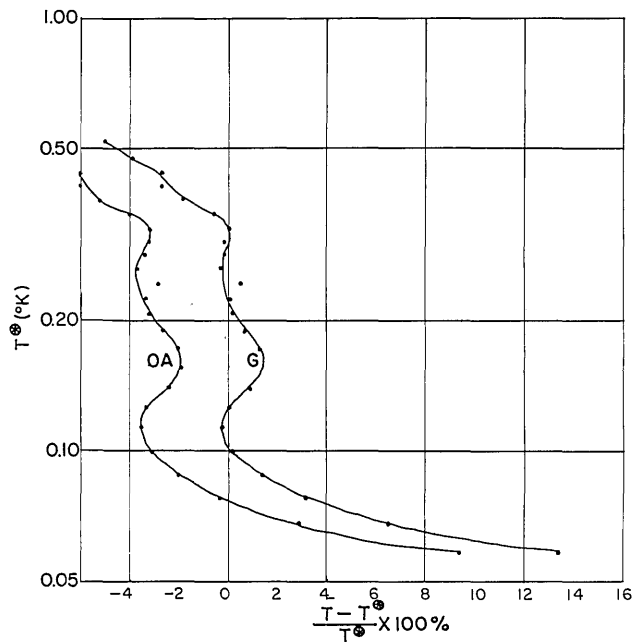


Fig. 13 - Results of the T^{\otimes} - T correlation (Run V). The percent deviation of the thermometer temperature from the magnetic temperature is plotted as a function of magnetic temperature. The symbol G indicates that the calibration for the thermometer, in the 4.2°K to 1.3°K range, was ignored. The symbols 0B and 1B indicate that the Curie plot was taken immediately before and one demagnetization before, respectively, the demagnetization under consideration.

Fig. 14 - Results of the T^{\otimes} - T correlation (Run V, Third Demagnetization). The percent deviation of the thermometer temperature from the magnetic temperature is plotted as a function of magnetic temperature. The symbol 0A refers to the Curie plot taken after the demagnetization under consideration.



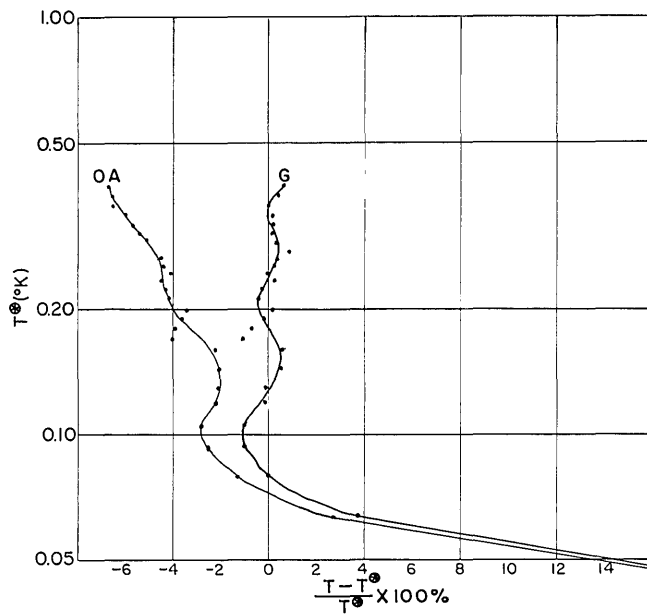


Fig. 15 - Results of the $T^{\otimes} - T$ correlation (Run VI, First Demagnetization). The percent deviation of the thermometer temperature from the magnetic temperature is plotted as a function of magnetic temperature.

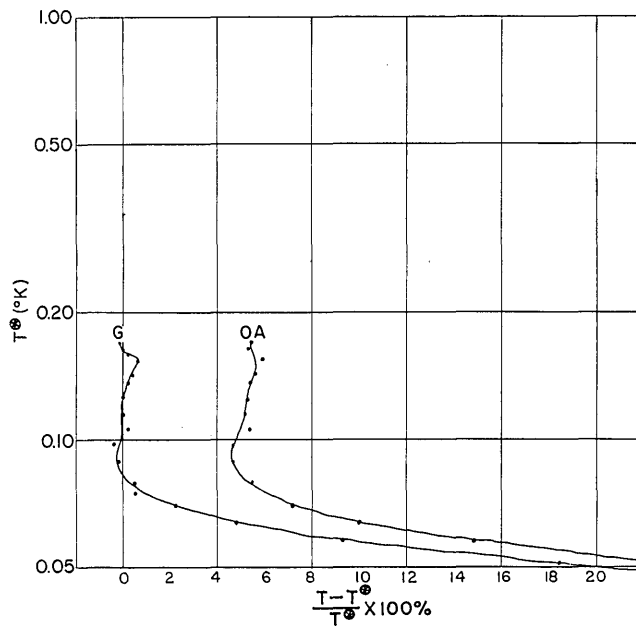


Fig. 16 - Results of the $T^{\otimes} - T$ correlation (Run VI, Second Demagnetization). The percent deviation of the thermometer temperature from the magnetic temperature is plotted as a function of magnetic temperature.

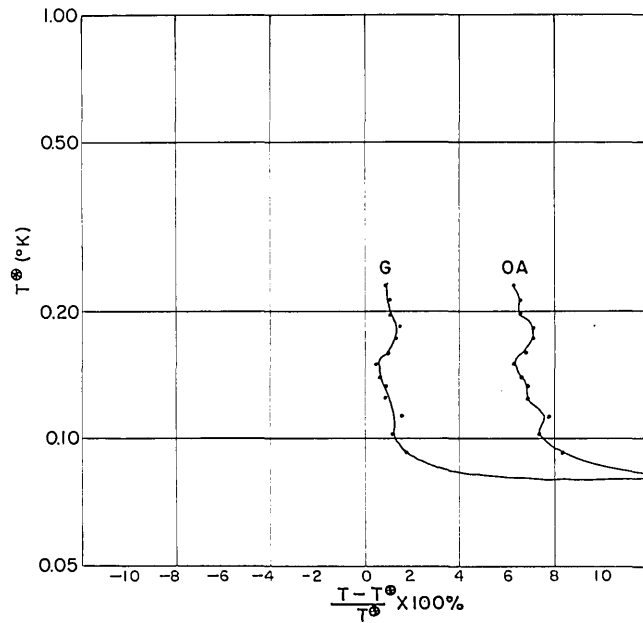


Fig. 17 - Results of the $T^{\otimes} - T$ correlation (Run VI, Third Demagnetization). The percent deviation of the thermometer temperature from the magnetic temperature is plotted as a function of magnetic temperature.

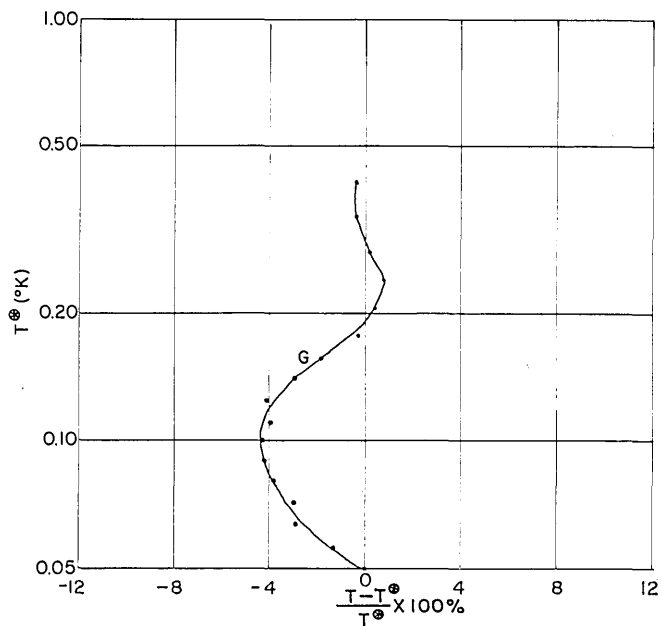


Fig. 18 - Results of the $T^{\otimes} - T$ correlation (Run VII, Second Demagnetization). The percent deviation of the thermometer temperature from the magnetic temperature is plotted as a function of magnetic temperature.

Table 3
 $T^{\circ} - T$ Correlation Data for Run VIII

Time (min)	$\text{Ce}(\text{PO}_3)_3$ T° ($^{\circ}\text{K}$)	CMN T_1 ($^{\circ}\text{K}$)	CMN T_2 ($^{\circ}\text{K}$)	CMN T_G ($^{\circ}\text{K}$)
2	0.00844	0.0197	0.0190	0.0210
16	0.00966	0.0216	0.0209	0.0230
29	0.0108	0.0226	0.0218	0.0241
44	0.0122	0.0237	0.0229	0.0253
57	0.0137	0.0243	0.0235	0.0259
66	0.0148	0.0249	0.0240	0.0265
85	0.0174	0.0261	0.0252	0.0278
104	0.0204	0.0276	0.0266	0.0294
122	0.0235	0.0291	0.0281	0.0310
137	0.0265	0.0306	0.0295	0.0326
150	0.0291	0.0318	0.0307	0.0339
153	0.0298	0.0321	0.0310	0.0342
170	0.0334	0.0340	0.0328	0.0362
221	0.0431	0.0404	0.0390	0.0430
232	0.0476	0.0428	0.0413	0.0456
245	0.0519	0.0460	0.0443	0.0489
259	0.0569	0.0500	0.0482	0.0531
265	0.0591	0.0518	0.0499	0.0550
279	0.0649	0.0566	0.0545	0.0600
297	0.0735	0.0644	0.0620	0.0682
312	0.0818	0.0717	0.0690	0.0759
333	0.0960	0.0850	0.0817	0.0899
343	0.1037	0.0923	0.0887	0.0974
360	0.1193	0.1079	0.1037	0.1138
372	0.1356	0.1242	0.1191	0.1307
380	0.1507	0.1381	0.1323	0.1449
404	0.2290	0.2156	0.2056	0.2238
424	0.3018	0.2977	0.2825	0.3055
443	0.4022	0.3966	0.3740	0.4014
454	0.4798	0.4764	0.4470	0.4770
465	0.5823	0.5827	0.5432	0.5752
471	0.6546	0.6573	0.6099	0.6424

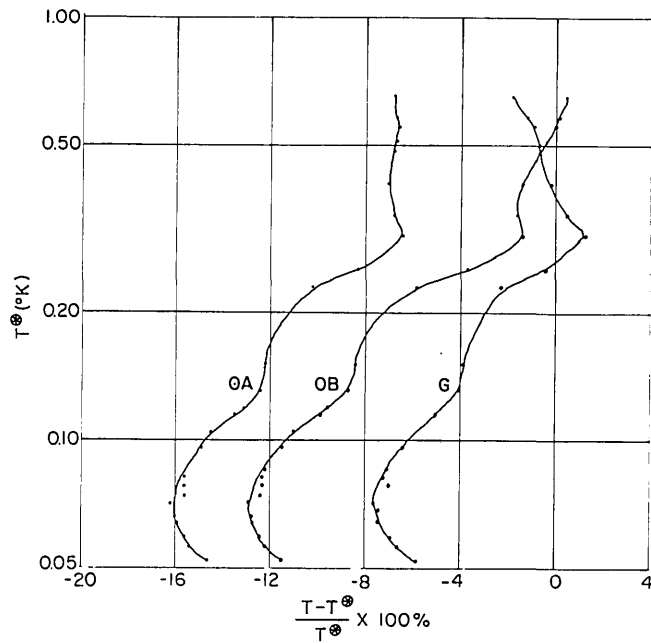


Fig. 19 - Results of the $T^{\oplus} - T$ correlation (Run VIII). The percent deviation of the thermometer temperature from the magnetic temperature is plotted as a function of magnetic temperature.

Warmup

The magnetic temperature of the 50% CBP glass is plotted against elapsed time in Figs. 20 through 23.

DISCUSSION OF RESULTS

Density

The measured density of the 50% CBP glass (3.57), compares well with the value 3.54 measured by Berger and Rubinstein (16) on cerous phosphate glass of composition $Ce_2O_3 \cdot 2.67 P_2O_5$.

Curie Constant

The Curie constant λ was measured as a sidelight in the adiabatic demagnetization experiments. The experiments, which yielded an approximate value for λ , were set up for good magnetic cooling performance rather than for accurate measurements of λ . The major uncertainty in the measured value of λ arises from the uncertainty in the actual amount of paramagnetic material in the slurries and from a 7.25% change in the slope of a Curie plot indicated by two sets of measurements on the same specimen.

It is instructive to compare the calculated value of λ with the experimental value. Using Eq. (21) with $g = 2$, one obtains a calculated value of $\lambda = 0.00194$. To calculate the lowest experimental estimate of $\lambda = 0.00189$, a value of $g = 1.974$ must be used. It appears that the lower experimental estimate of λ is consistent with that calculated using Eq. (21).

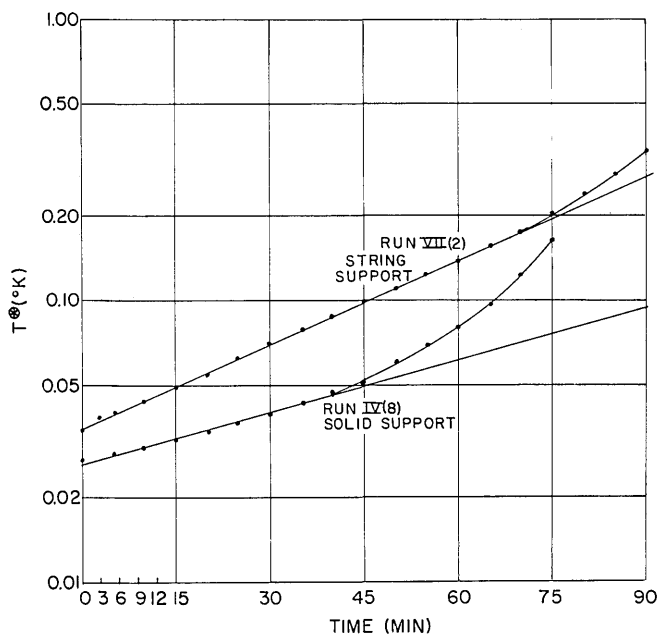


Fig. 20 - Warmup after demagnetization. The magnetic temperature is plotted as a function of elapsed time. The number in parentheses indicates the particular demagnetization to which the data apply.

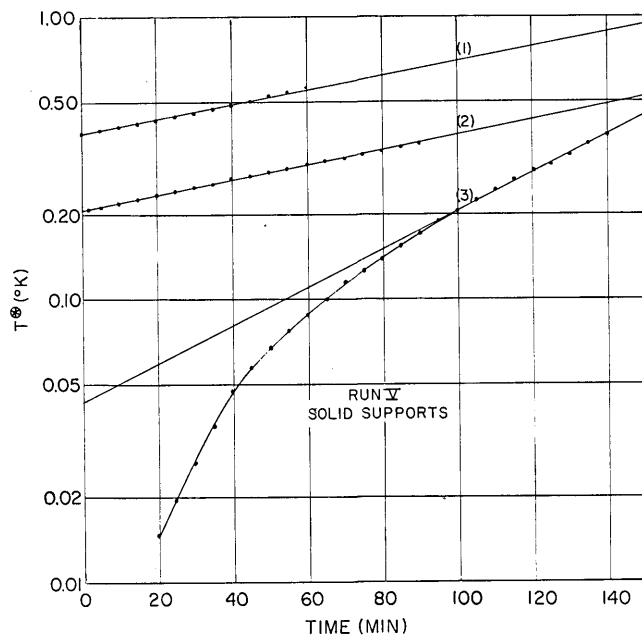


Fig. 21 - Warmup after demagnetization. The magnetic temperature is plotted as a function of elapsed time. The number in parentheses indicates the particular demagnetization to which the data apply.

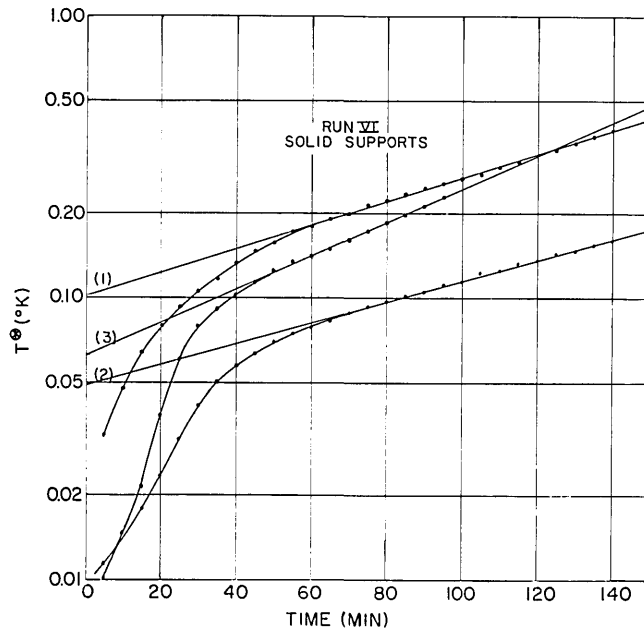


Fig. 22 - Warmup after demagnetization. The magnetic temperature is plotted as a function of elapsed time. The number in parentheses indicates the particular demagnetization to which the data apply.

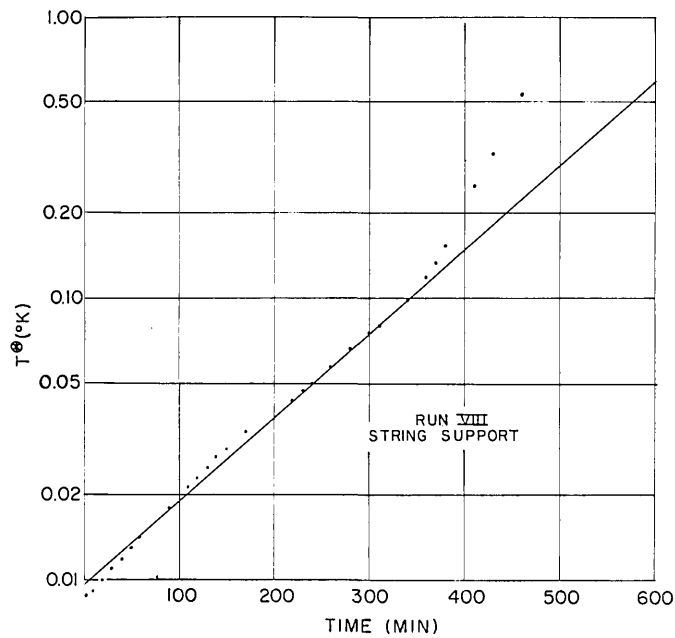


Fig. 23 - Warmup after demagnetization. The magnetic temperature is plotted as a function of elapsed time. The number in parentheses indicates the particular demagnetization to which the data apply.

Temperatures Produced from Different H/T 's

The graph in Fig. 11 shows that the glass is capable of producing magnetic temperatures well below 0.01°K . The absolute temperature of the glass corresponding to a given magnetic temperature near 0.01°K is open to question. For most of the hydrated salts mentioned in Table 1, the absolute temperature is always lower than T^\otimes . However, T is greater than T^\otimes for copper potassium sulfate, because its susceptibility obeys a Curie-Weiss law, $\chi \propto (T - \Delta)^{-1}$, with $\Delta = 0.034$ (19).

The existence of a small Curie-Weiss Δ for the cerium glass cannot be inferred from the ballistic galvanometer measurements in the liquid helium temperature range. The galvanometer deflection is given by

$$\delta = A(T - \Delta)^{-1} + \delta_0, \quad (36)$$

or

$$\frac{1}{\delta - \delta_0} = \frac{T}{A} - \frac{\Delta}{A},$$

where δ_0 is the galvanometer deflection for no specimen ($x = 0$). Many sets of the variables A , Δ , and δ_0 will satisfy the straight-line equation, Eq. (36) (within experimental scatter), using the same δ -versus- T data. An apparatus which either eliminates or allows an independent measurement of δ_0 must be used to obtain a reliable estimate of Δ .

Depending upon whether the deviation from simple Curie law behavior is in the ferromagnetic sense or in the antiferromagnetic sense, the absolute temperature will be greater than or less than T^\otimes , respectively.

In Fig. 12, T_f^\otimes was plotted as a function of T_i/H to illustrate the applicability of Eq. (12). The very large intercept is not in good agreement with Eq. (12), which indicates that the data for $T_i/H < 0.13^\circ\text{K/kOe}$ (Kurti-Simon condition) should lie on a straight line which extrapolates through zero.

The existence of the large intercept (-0.125°K) in Fig. 12 can be interpreted in one of two ways, both involving the concept of dipole interaction: (a) the existence of a Curie-Weiss Δ , due to dipole-dipole and exchange interactions, which when added to the magnetic temperature yields the true thermodynamic temperature, or (b) failure of Eq. (12) due to considering the effective dipole-dipole interaction equivalent to an effective applied field of magnitude h .

Consider the former possibility. Although the following analysis, valid only for small H/T , is not applicable to the experimental data ($H/T \geq 1$), its perusal is instructive because it shows that the existence of Curie-Weiss behavior in the susceptibility predicts an intercept similar to that in Fig. 12, and because a more general analysis valid for $H/T \geq 1$ is complicated beyond manageability.

The entropy of a magnetic system is a function of H and T . Therefore,

$$dS = \left(\frac{\partial S}{\partial T}\right)_H dT + \left(\frac{\partial S}{\partial H}\right)_T dH, \quad (37)$$

or

$$dS = \frac{C_H}{T} dT + \left(\frac{\partial m}{\partial T}\right)_H dH,$$

where the Maxwell relation

$$\left(\frac{\partial S}{\partial H}\right)_T = \left(\frac{\partial m}{\partial T}\right)_H$$

was used. In the limit when $g\beta H \ll kT$ the Curie-Weiss magnetization is given by

$$m = \chi H = \lambda' H / (T - \Delta) \quad (38)$$

and

$$\left(\frac{\partial m}{\partial T}\right)_H = -\lambda' H / (T - \Delta)^2. \quad (39)$$

The heat capacity is itself a function of H and T . Assuming that the final temperatures reached after demagnetization are large in comparison to the interaction temperature θ , the zero field heat capacity of the system will vary as T^{-2} in accordance with Eq. (28). Appendix A amends Eq. (28) to include magnetic field dependence for small H/T . The result is

$$C_H(H, T) = \lambda h^2 / T^2 + \lambda' T H^2 / (T - \Delta)^3. \quad (40)$$

Therefore, after insertion of the Eqs. (39) and (40) into Eq. (37), the entropy of the system is

$$\int dS = \lambda h^2 \int \frac{dT}{T^3} + \lambda' \int \frac{H^2}{(T - \Delta)^3} dT - \lambda' \int \frac{H}{(T - \Delta)^2} dH.$$

The second and third integrals on the right side can be combined so that the entropy expression becomes

$$\int dS = \lambda h^2 \int \frac{dT}{T^3} - \frac{\lambda'}{2} \int d \left[\frac{H^2}{(T - \Delta)^2} \right]$$

or

$$S(H, T) - S(0, \infty) = -\frac{\lambda h^2}{2T^2} - \frac{\lambda' H^2}{2(T - \Delta)^2}. \quad (41)$$

The entropy change for isentropic demagnetization from (H_i, T_i) to $(0, T_f)$ is zero. Therefore,

$$\lambda h^2 (T_f^{-2} - T_i^{-2}) = \lambda' H_i^2 / (T_i - \Delta)^2. \quad (42)$$

Imposing the change of variable $T^\circledast = T - \Delta$, and noting that usually $1/T_f^2 \gg 1/T_i^2$, one has

$$\lambda h^2 / (T_f^\circledast + \Delta)^2 \approx \lambda' H_i^2 / T_i^2$$

or

$$T_f^\circledast \approx k(\lambda/\lambda')^{1/2} T_i / H_i - \Delta. \quad (43)$$

Equation (43) shows that a plot of T^\circledast versus T_i/H_i for $g\beta H_i/kT_i \ll 1$ has an intercept equal to the Curie-Weiss Δ . Since T_f^\circledast is obtained from extrapolation of the Curie (or Curie-Weiss) plot calibration taken at liquid helium temperatures, the same value of Δ must be used in the calibration as is obtained by the intercept. The value of Δ used in

the plot of δ versus $(T - \Delta)^{-1}$ must not introduce curvature, because this would violate the hypothesis of Curie-Weiss behavior.

There are several objections to applying Eq. (43) to the experimental data for the 50% CBP glass. The condition $g\beta H_i/kT_i \ll 1$ is not satisfied for any of the experimental points, and the generalization of Eq. (43) for large $g\beta H/kT$ is not straightforward. Furthermore, the assumption $1/T_f^2 \gg 1/T_i^2$ is not well satisfied, so that

$$\left[(T_f^{\otimes} + \Delta)^{-2} - (T_i^{\otimes} + \Delta)^{-2} \right]^{-1/2}$$

must be plotted against T_i/H_i with a value of Δ such that there is zero intercept.

Overlooking the first objection, but correcting for the second, one obtains $\Delta = 0.156^\circ\text{K}$ (Fig. 24). However, five out of seven Curie-Weiss plots taken between 4.2°K and 1.3°K with $\Delta = 0.156^\circ\text{K}$ showed small but definite curvature with the same sense of concavity. In the other two Curie-Weiss plots curvature could not be distinguished from scatter in the data. The corresponding Curie plots with shape correction only, $\Delta = 0.002^\circ\text{K}$, showed no observable curvature. A contradiction has arisen in the value of Δ required to satisfy Eq. (43) and the value required to preserve linearity in the Curie plots.

Although 16 Curie plots were taken during seven different runs, only seven of the plots span the temperature range 4.2°K to 1.3°K . The remaining plots span the

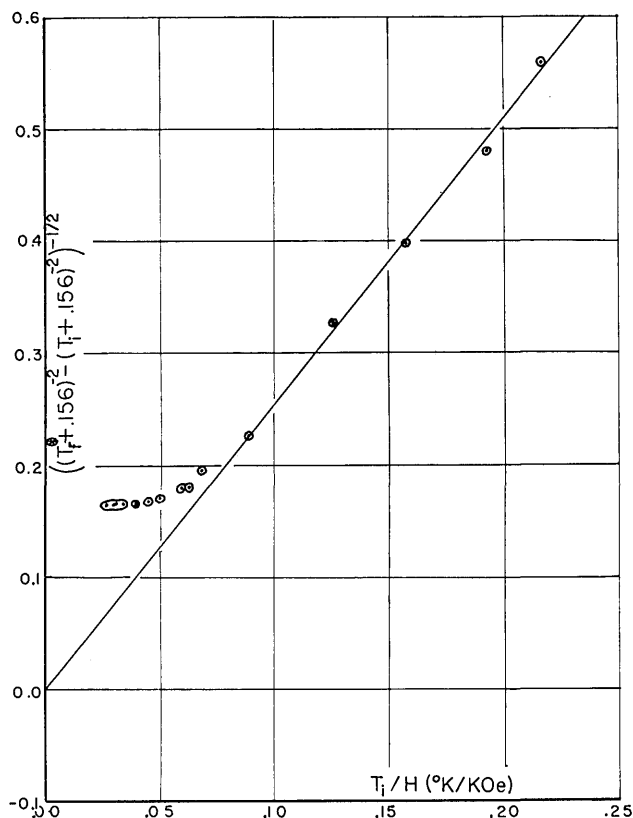


Fig. 24 - Graph of the experimental T_f^{\otimes} versus T_i/H data for a Curie-Weiss Δ equal to 0.156°K

temperature range from 2.17°K (lambda point) to 1.3°K . The thermal conductivity of liquid helium above the lambda point is so poor that large temperature inhomogeneities may exist in a helium bath when it is allowed to warm from below the lambda temperature to 4.2°K . The bottom of the bath remains colder than the top. However, when the temperature of the bath is initially lowered from 4.2°K , convectional currents wipe out thermal inhomogeneities. Below the lambda point the thermal conductivity of liquid helium II is very good, and Curie plots may be taken by either increasing or decreasing the bath temperature. Unfortunately, the data taken below the lambda point do not span a large enough temperature difference to clearly expose curvature.

Referring again to Fig. 12, the deviation of the data from linearity at small T° is probably due to the onset of strong magnetic interaction. Similar behavior is observed for CMN (Fig. 25).

T° - T Correlation

The results of the T° - T correlation experiments are shown in Figs. 13 through 19. The symbols 0B, 1B, 2B, ... indicate that the Curie plot was taken either immediately before, one demagnetization before, two demagnetizations before, ... the demagnetization under consideration. The symbols 0A, 1A, 2A, ... refer to Curie plots taken after the demagnetization under consideration. The symbol G indicates that the calibration for the thermometer, taken in the 4.2°K to 1.3°K temperature range, was ignored for reasons

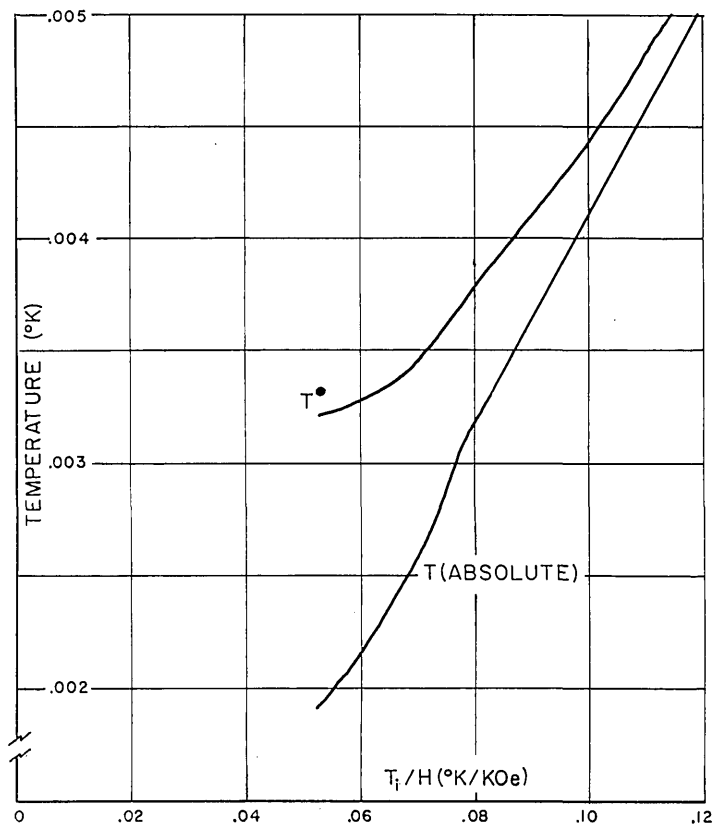


Fig. 25 - Absolute and magnetic temperatures of cerous magnesium nitrate as a function of T_i/H . The data were taken from Ref. 1.

to be discussed, and that an alternative calibration was obtained by fitting the galvanometer deflections for the CMN thermometer to the corresponding $1/T^{\otimes}$ values for the glass at relatively large values of T^{\otimes} . It was assumed that at high enough temperatures T^{\otimes} and T must be identical. In some instances, A , B , and G calibrations are applied to the same set of data, and the resulting curves are plotted on the same graph for comparison.

The Curie plot for the CBP glass seldom varied more than a few percent during the series of demagnetizations conducted on a given day. On the other hand, the Curie plot for the CMN thermometer invariably changed a minimum of 4% between successive observations. The calibration change is attributed to movement of the CMN specimen relative to the susceptibility coils, this movement being initiated by the nonuniform stray field in the magnetization process. When no Curie plot was taken immediately before or after the demagnetization, and the Curie plots taken earlier or later appear obviously inconsistent with the data, the G calibrations are the only means of interpreting the data.

At the low-temperature end all the curves show rapidly increasing positive deviations, indicating that the thermometer is becoming increasingly hotter than the magnetic temperature of the glass. Since the rapid increase occurs at lower temperatures in the runs with longer warmup time (smaller heat leak), the deviation is interpreted as deterioration of thermal contact between the glass and the thermometer. Implications of the data in this temperature range should be considered cautiously.

With the exception of the data from run VIII, the magnetic temperature of the 50% CBP glass agrees with the temperature of the thermometer within $\pm 8\%$ down to 0.1°K . The data from run VIII extends the deviation to a maximum of -14% at 0.1°K , but the A and B curves appear somewhat inconsistent with the earlier observations. Considering the G curves only, all the data indicate that, down to 0.1°K , T^{\otimes} is equal to the temperature of the CMN thermometer within $\pm 6\%$.

A portion of the correlation data for run VIII is presented in Table 3. Temperatures of the CBP glass and CMN thermometer are simultaneously presented as a function of elapsed time. Three values of thermometer temperature are presented, corresponding to the initial and final CMN Curie plots and the graphical fit described earlier. From the three sets of temperature values one can estimate the degree of uncertainty of the CMN temperature. Although on a percentage basis the agreement between the temperatures of the CBP glass and the CMN thermometer is poor, the very fact that the two temperatures follow each other approximately for 471 min (almost 8 hours) suggests a reasonable degree of thermal contact between the glass and the thermometer.

The data from run VIII indicate that 2 min after the demagnetization the temperature of the thermometer was about 0.02°K . The thermometer could have been cooled to this temperature in two ways: (a) the CBP glass did cool to about 0.02°K upon demagnetization and the thermometer was cooled by thermal contact, and (b) the stray field from the magnet cooled the CMN thermometer to 0.02°K upon demagnetization, and supposing the thermal contact to be poor, the temperature of the thermometer is independent of the glass. In this case the temperature of the glass could be much different from that of the thermometer.

There is evidence that case (b) must be refuted. Observe that after 295 min (almost 5 hours) the thermometer temperature rose to about 0.063°K . If the thermometer was really thermally isolated from the CBP glass, then it is a simple matter to calculate the average (constant) heat leak responsible for this rise in temperature. The heat capacity of CMN is given (4) approximately by

$$C/Nk = 5.76 \times 10^{-6}/T^2. \quad (44)$$

The thermometer consisted of about 12.7 g of CMN, therefore

$$C = 8.02/T^2 \text{ erg}/^\circ\text{K}. \quad (45)$$

The average or constant heat leak into the thermometer responsible for a change in temperature from T_1 to T_2 in time t is given by

$$\dot{Q} = \frac{8.02}{t} \left(\frac{1}{T_1} - \frac{1}{T_2} \right) \text{ erg/unit time}. \quad (46)$$

For $T_1 = 0.02^\circ\text{K}$, $T_2 = 0.063^\circ\text{K}$, and $t = 295$ min, one calculates $\dot{Q} = 0.93$ erg/min. This extremely minute heat leak is at least 25 times smaller than heat leaks obtained with similar apparatus by other workers in this laboratory. On the basis that such a small heat leak is absurd for the apparatus used, it can be concluded that the CMN thermometer and CBP glass could not have been completely thermally isolated.

If one assumes that the thermal contact between glass and thermometer is adequately described by the T^3 law, Eq. (35), then it is possible to calculate the amount of time t required for the thermometer to rise in temperature from T_0 to T' because of thermal contact with the glass at temperature T_1 , where $T_1 > T'$ and T_0 . In Appendix B the necessary relation between t , T_1 , T_0 , and T' is derived for the case in which T_1 is a constant-temperature reservoir. The amount of time was calculated for the thermometer to warm from 0.0193°K to 0.076°K (which took about 5 hours in run VIII) for various values of $T_1 > 0.076^\circ\text{K}$. The following results were found: for $T_1 = 0.20^\circ\text{K}$, $t = 0.32$ sec, for $T_1 = 0.10^\circ\text{K}$, $t = 2.7$ sec, and for $T_1 = 0.08^\circ\text{K}$, $t = 6.2$ sec.

One concludes that if the CBP glass cooled to only 0.1°K or 0.2°K after isentropic demagnetization (which would be the case if the susceptibility obeyed a Curie-Weiss law with $\Delta \approx 0.15^\circ\text{K}$) while the thermometer cooled to about 0.02°K , then the thermometer would warm through 0.076°K in a matter of seconds rather than the 5 hours it took in run VIII.

The preceding arguments have been presented as convincing evidence that the thermometer is actually following the temperature of the glass. On this basis, the 50% CBP glass is capable of cooling to around 0.02°K . A more sophisticated technique, such as described in Appendix C, is required to establish a detailed temperature scale below 0.1°K .

Warmup

Figures 20 to 23 show the increase of magnetic temperature of the CBP glass after demagnetization as a function of elapsed time. A logarithmic temperature scale was used as a matter of convenience.

An attempt was made to fit the time dependence of the warmup data to that expected for a T^{-2} heat capacity and constant heat leak \dot{Q} . (The temperature dependence of \dot{Q} is almost negligible below 0.5°K according to the T^3 law.) If the heat capacity of the CBP glass is given by $C = A/T^2$ and the relationship between magnetic and absolute temperatures is given by $T = T^\circ + \Delta$, then, for a constant heat leak,

$$\frac{1}{T^\circ + \Delta} = -\frac{\dot{Q}t}{A} + \frac{1}{T_0}. \quad (47)$$

A plot of $(T^{\otimes} + \Delta)^{-1}$ against elapsed time should yield a straight line with negative slope, if the appropriate value of Δ is added to T^{\otimes} . The values of Δ required to yield linearity in Eq. (47) for some of the warmups on the same specimen are: for run VIII,* $\Delta = 0.036^{\circ}\text{K}$; for run VII,* $\Delta = 0.068^{\circ}\text{K}$; for run VI, $\Delta = 0.500^{\circ}\text{K}$; and for run V, $\Delta = 0.319^{\circ}\text{K}$.

This method of determining Δ was abandoned, since the results lacked consistency. However, it is interesting to note that the smallest value of Δ corresponds to run VIII which had the smallest heat leak. Intermittant vibrational heating of the specimen due to transferred building vibrations is a possible explanation of the inconsistency in the value of Δ . Vibrational heating would be expected to be more of a problem in runs V and VI where the dewar rested directly on the magnet instead of being suspended like a pendulum from the ceiling. Obviously if \dot{Q} is not constant, allowing T^{\otimes} to vary unpredictably with time, a large enough value of Δ will mask the T^{\otimes} variation such that an almost linear (although very flat) curve will result when $(T^{\otimes} + \Delta)^{-1}$ is plotted versus t . It is the author's opinion that this is what occurs in runs V and VI.

SUMMARY

The 50% CBP glass was successfully demagnetized to magnetic temperatures as low as 0.0069°K . A plot of the magnetic temperature reached after isentropic demagnetization from various T_i/H values in accordance with Eq. (12) yielded a rather large intercept with the possible implication of a Curie-Weiss Δ of 0.156°K . A Curie-Weiss Δ of this magnitude was found to be inconsistent with the Curie plots taken in the liquid helium temperature range, since curvature would result in the majority of cases. The $T^{\otimes}-T$ correlation experiments indicated that the CBP glass cooled to an absolute temperature of roughly 0.02°K ($T^{\otimes} = 0.0084^{\circ}\text{K}$). This also fails to support $\Delta = 0.156^{\circ}\text{K}$, since a paramagnetic material will not usually cool much lower than the temperature corresponding to its Curie-Weiss Δ . The large intercept in Fig. 12 is thus attributed to the failure of the simple theory to correctly account for intrinsic magnetic interactions. Observation of the warmup after demagnetization yielded no consistent value of Δ .

With the exception of the data from run VIII, the temperature of the glass agrees with the temperature of the thermometer to within $\pm 8\%$ down to 0.1°K . The data from run VIII increases the deviation to a maximum of -14% at 0.1°K .

Within experimental error, the measured value of the Curie constant is consistent with the value calculated from Eq. (21) with $J = 1/2$ and $2 \geq g \geq 1.974$.

ACKNOWLEDGMENTS

This report was originally written as a master of science thesis for the University of Maryland.

I acknowledge the help and advice of Dr. G. T. Rado of the Naval Research Laboratory as an advisor on the work. In addition, I thank Dr. D. A. Spohr for suggesting the topic, for helping to record the data, and for many helpful discussions. I also thank Dr. R. A. Hein for the use of his equipment, and Mrs. M. L. Etzel for typing the manuscript. I am especially indebted to the Naval Research Laboratory for the use of its facilities and for encouragement to pursue a graduate education while serving as an employee.

*In these warmups the specimen was hung from a cotton thread instead of being mounted on the graphite rods. Also, the dewar was suspended on a rope from the ceiling instead of resting on the magnet.

REFERENCES

1. Frankel, R.B., Shirley, D.A., and Stone, N.J., Phys Rev. 140:1020-1023 (1965)
2. deKlerk, D., Handbuch der Physik, Berlin:Springer-Verlag, Vol. 15, 1956, p. 38
3. Hudson, R.P., Kaeser, R.S., and Radford, H.E., Proceedings of the VII International Conference on Low-Temperature Physics, Canada:University of Toronto Press, 1961, pp. 100-106
4. Hudson, R.P., and Kaeser, R.S., Physics 3:(No. 2):95-113 (1967)
5. Sachs, M., "Solid State Theory," New York:McGraw-Hill, 1963, p. 122
6. Kurti, N., and Simon, F., Proc. Roy. Soc. (London) 149:152-76 (1935)
7. Bethe, H., Ann. Phys. 3(No. 5):133 (1929)
8. Garrett, C.G.B., "Magnetic Cooling," New York:Wiley, 1954, p. 46
9. Hoare, F.E., Jackson, L.C., and Kurti, N., "Experimental Cryophysics," London: Butterworth and Co., Ltd., 1961, pp. 197-201
10. Parks, R.D., Proceedings of the VIII International Conference on Low Temperature Physics, London:Butterworth and Co., Ltd., 1963, pp. 427-429
11. Pal, L., Tarnoczi, T., and Nemeth, G., Brit. J. Appl. Phys. 14:212-14 (1963)
12. White, G.K., "Experimental Techniques in Low-Temperature Physics," Oxford: Clarendon Press, 1959, pp. 227-229
13. Joseph, R.I., J. Appl. Phys. 37:4639-43 (1966)
14. Nicol, J., and Tseng, T.P., Phys. Rev. 92:1062-63 (1953)
15. Alers, P.B., Phys. Rev. 116:1483 (1959)
16. Berger, S.B., and Rubinstein, C.B., J. Appl. Phys. 35:1798-1801 (1964)
17. Spohr, D.A., "Experiments on the Orientation of Nuclei at Temperatures Near the Absolute Zero," unpublished Ph.D. Thesis, Oxford, 1958, pp. 49-50
18. Shore, F.J., Sailor, V.L., Marshak, H., and Reynolds, C.A., Rev. Sci. Instr. 31:970-3 (1960)
19. Garrett, C.G.B., Proc. Roy. Soc. (London) A203:375-91 (1950)
20. Beun, J.A., Miedma, A.R., and Steenland, M.J., Physica 23:1-25 (1957)
21. Daniels, J.M., and Kurti, N., Proc. Roy. Soc. (London) A221:243-256 (1954)

Appendix A

MAGNETIC FIELD DEPENDENCE OF THE HEAT CAPACITY

Using thermodynamics it is easy to show that the variation of the heat capacity with magnetic field is given by

$$\left(\frac{\partial C_H}{\partial H}\right)_T = T \left(\frac{\partial^2 \mathfrak{M}}{\partial T^2}\right)_H, \quad (\text{A1})$$

where, as before, it is understood that the system has no pressure-volume dependence. In accordance with the expression for the Curie-Weiss magnetization given in Eq. (38), one has

$$\left(\frac{\partial^2 \mathfrak{M}}{\partial T^2}\right)_H = \frac{2\lambda'H}{(T-\Delta)^3}. \quad (\text{A2})$$

Integrating partially with respect to H (constant T), the heat capacity is given by

$$C_H(H, T) = \lambda'TH^2/(T-\Delta)^3 + f(T). \quad (\text{A3})$$

The function $f(T)$ is evaluated by requiring that the heat capacity be given by Eq. (28) when $H=0$. Thus,

$$f(T) = \lambda h^2/T^2. \quad (\text{A4})$$

The heat capacity, as a function of H and T , is then given by

$$C_H(H, T) = \lambda h^2/T^2 + \lambda'TH^2/(T-\Delta)^3. \quad (\text{A5})$$

It must be remembered that the above equation is valid as long as the magnetic field is small enough such that Eq. (38) accurately describes the magnetization and as long as the temperature is high enough such that Eq. (28) accurately describes the zero-field heat capacity.

Appendix B

TIME RESPONSE OF THE CMN THERMOMETER AS DETERMINED BY THE T^3 THERMAL CONTACT LAW

Consider the situation where a known quantity of CMN, used as a thermometer, is connected thermally to a constant-temperature reservoir at temperature T_1 by a highly conducting heat link. It will be assumed that the thermal impedance of the heat link is always small enough to be neglected in comparison to that presented by contact resistances between the heat link and the CMN and the heat link and the reservoir. Assuming that the CMN is initially colder than T_1 , the rate of flow of heat is given by

$$\dot{Q} = \xi A' (T_1^3 - T^3), \quad (\text{B1})$$

in accordance with Eq. (35), where T is the instantaneous temperature of the CMN. The rate at which T increases with time is determined by the heat capacity of CMN, which is given by

$$C = \dot{Q} \frac{dt}{dT} = \xi A' (T_1^3 - T^3) \frac{dt}{dT}. \quad (\text{B2})$$

In accordance with Eq. (44), $C = B/T^2$. Therefore,

$$\frac{\xi A' t}{B} = \int_{T_0}^{T'} \frac{dT}{T^2 (T_1^3 - T^3)}, \quad (\text{B3})$$

where T_0 is the value of T at $t = 0$, and T' is the temperature at some arbitrary time t . The integral is readily evaluated by available integration formulas, with the result that

$$\frac{\xi A' t}{B} = - \left. \frac{1}{T_1^3 T} \right]_{T_0}^{T'} + \frac{1}{3T_1^4} \left[\frac{1}{2} \ln \frac{(T^3 - T_1^3)}{(T - T_1)^3} + \sqrt{3} \tan^{-1} \frac{(2T + T_1)}{-\sqrt{3} T_1} \right]_{T_0}^{T'}. \quad (\text{B4})$$

This equation allows one to compute the amount of time t for the CMN thermometer to warm from T_0 to T' when connected to a reservoir at temperature T_1 . Note that, in this analysis, an infinite amount of time is required to warm from T_0 to $T' = T_1$, since the rate of heat flow is dependent upon the existence of a temperature difference between the reservoir and the CMN thermometer.

Appendix C

ABSOLUTE DETERMINATION OF THE TEMPERATURE SCALE FOR A PARAMAGNETIC MATERIAL

The following scheme allows one to determine the absolute temperature corresponding to a given magnetic temperature. Let T^{\otimes} indicate the magnetic temperature measured at a given time after demagnetization. One can experimentally measure an $S-T^{\otimes}$ curve. An amount of entropy S_1 is removed from the system by isothermally magnetizing at $T = T_0^{\otimes} = T_0$ (absolute — since Curie's law is obeyed here), and a magnetic temperature T^{\otimes} is measured upon adiabatic demagnetization. By successive demagnetizations with successively higher entropy removals, the $S-T^{\otimes}$ curve can be plotted. In theory — although it is difficult in practice — the amount of entropy removed can be calculated from the amount of helium boiloff from the 1°K bath as the heat of magnetization is isothermally absorbed. The relation is $\Delta S = \Delta Q/T_{\text{helium bath}}$. The quantity ΔQ is calculated from the observed quantity of helium gas evolved and the known heat of vaporization.

One then makes heat capacity measurements over small temperature intervals from the lowest temperature to liquid helium temperatures by heating the paramagnetic material by a small known quantity ΔQ and observing the magnetic temperature difference T^{\otimes} . (Gamma-ray irradiation is the best known method of heating the salt, since it produces uniform heating; electrical heating often produces local heating.) The applicable equations are

$$C_H = T \left(\frac{\partial S}{\partial T} \right)_H = T \left(\frac{\partial S}{\partial T^{\otimes}} \right)_H \left(\frac{\partial T^{\otimes}}{\partial T} \right)_H = \left(\frac{dQ}{dT^{\otimes}} \right)_H \left(\frac{\partial T^{\otimes}}{\partial T} \right)_H \quad (C1)$$

and

$$\left(\frac{dQ}{dT^{\otimes}} \right)_H = T \left(\frac{\partial S}{\partial T^{\otimes}} \right)_H \quad (C2)$$

The quantity ΔQ can be calculated from the conditions of gamma-ray irradiation; therefore,

$$T \approx \frac{\Delta Q}{\Delta T^{\otimes}} \left/ \left(\frac{\partial S}{\partial T^{\otimes}} \right)_H \right. , \quad (C3)$$

where

$$\Delta T^{\otimes} = T_1^{\otimes} - T_2^{\otimes} ,$$

$$T^{\otimes} = (T_2^{\otimes} + T_1^{\otimes}) / 2 ,$$

T_1^{\otimes} and T_2^{\otimes} are the initial and final magnetic temperatures upon gamma-ray heating,

ΔQ and ΔT^{\otimes} are small quantities,

$(\partial s / \partial T^{\circledast})_H$ is evaluated from the slope of the $s-T^{\circledast}$ curve,

and Eq. (C3) is evaluated with $H=0$.

A technique of correlating a given magnetic temperature T^{\circledast} with its thermodynamic temperature T has thus been established.

DOCUMENT CONTROL DATA - R & D

(Security classification of title, body of abstract and indexing annotation must be entered when the overall report is classified)

1. ORIGINATING ACTIVITY (Corporate author) Naval Research Laboratory Washington, D.C. 20390		2a. REPORT SECURITY CLASSIFICATION Unclassified	
		2b. GROUP	
3. REPORT TITLE THE PRODUCTION OF TEMPERATURES BELOW 1° K BY THE ADIABATIC DEMAGNETIZATION OF 50% Ce(PO ₃) ₃ -Ba(PO ₃) ₂ GLASS			
4. DESCRIPTIVE NOTES (Type of report and inclusive dates) A final report on the problem. Unless otherwise notified the problem will be considered closed 30 days after the issuance of this report.			
5. AUTHOR(S) (First name, middle initial, last name) Edwin Lewis Althouse			
6. REPORT DATE July 15, 1968		7a. TOTAL NO. OF PAGES 45	7b. NO. OF REFS 21
8a. CONTRACT OR GRANT NO. NRL Problem P05-02		9a. ORIGINATOR'S REPORT NUMBER(S) NRL Report 6711	
b. PROJECT NO. RR 002-10-45-5051		9b. OTHER REPORT NO(S) (Any other numbers that may be assigned this report)	
c.			
d.			
10. DISTRIBUTION STATEMENT This document has been approved for public release and sale; its distribution is unlimited.			
11. SUPPLEMENTARY NOTES		12. SPONSORING MILITARY ACTIVITY Department of the Navy (Office of Naval Research), Washington, D.C. 20360	
13. ABSTRACT The technique of adiabatic demagnetization, also known as "magnetic cooling," for producing low temperatures has been in existence since 1933. Over the years a multitude of coolant materials has been discovered, but most of them are in the form of hydrated paramagnetic salts. Nonhydrous materials have the advantage of greater chemical stability; however, to the author's knowledge, none of the few non-hydrous paramagnetic materials previously investigated are capable of producing temperatures below 0.1° K. It was the object of this investigation to determine whether cerium metaphosphate glass (specifically 50% by weight Ce(PO ₃) ₃ -Ba(PO ₃) ₂) is a suitable coolant material for adiabatic demagnetization experiments. Cerium glass is not susceptible to dehydration and attack by glycerine (used for thermal contact) as are many of the hydrated salts. In addition, the concentration of magnetic atoms can be varied over a wide range by diluting the magnetic glass Ce(PO ₃) ₃ with the nonmagnetic glass Ba(PO ₃) ₂ . The principal results of this investigation are: (a) the 50% Ce(PO ₃) ₃ -Ba(PO ₃) ₂ glass was successfully cooled many times by adiabatic demagnetization, and (over)			

14. KEY WORDS	LINK A		LINK B		LINK C	
	ROLE	WT	ROLE	WT	ROLE	WT
Adiabatic demagnetization Low-temperature physics Cerium glass Paramagnetic materials						
<p>"magnetic" temperatures as low as 0.0069°K were reached, (b) using a cerium magnesium nitrate paramagnetic salt as a thermometer, absolute temperatures as low as 0.02°K were observed, and (c) within experimental error, the measured Curie constant for the cerium glass (density 3.57) agrees with that calculated from the Brillouin function for $J = 1/2$ and $1.97 \leq g \leq 2.00$.</p>						